energies

MDPI

Article

Hybrid Energy Routing Approach for Energy Internet

Sara Hebal [1], Djamila Mechta [1], Saad Harous [2,*] and Mohammed Dhriyyef [3]

[1] LRSD Laboratory, Computer Science Department, Ferhat ABBAS Sétif 1 University, 19000 Sétif, Algeria; sara.hebal@univ-setif.dz (S.H.); mechtadjamila@univ-setif.dz (D.M.)
[2] College of Information Technology, United Arab Emirates University, Al Ain 15551, United Arab Emirates
[3] Smart ICT Laboratory, National School of Applied Sciences, Mohammed First University, 60000 Oujda, Morocco; m.dhriyyef@ump.ac.ma
* Correspondence: harous@uaeu.ac.ae

Abstract: The Energy Internet (EI) has been proposed as an evolution of the power system in order to improve its efficiency in terms of energy generation, transmission and consumption. It aims to make the use of renewable energy effective. Herein, the energy router has been considered the crucial element that builds the net structure between the different EI components by connecting and controlling the bidirectional power and data flow. The increased use of renewable energy sources in EI has contributed to the creation of a new competitive energy trading market known as peer-to-peer energy trading, which enables each component to be part of the trading process. As a consequence, the concept of energy routing is increasingly relevant. In fact, there are three issues that need to be taken into account during the energy routing process: the subscriber matching, the energy-efficient path and the transmission scheduling. In this work, we first proposed a peer-to-peer energy trading scheme to ensure a controllable and reliable EI. Then, we introduced a new energy routing approach to address the three routing issues. A subscriber matching mechanism is designed to determine which producer/producers should be assigned for each consumer by optimizing the energy cost and transmission losses. This mechanism provides a solution for both mono and multi-source consumers. An improved ant colony optimization-based energy routing protocol was developed to determine a non-congestion minimum loss path. For the multi-source consumer case, an energy particle swarm optimization algorithm was proposed to choose a set of producers and to decide the amount of energy that should be collected from each producer to satisfy the consumer request. Finally, the performance of the proposed protocol, in terms of power losses, cost and computation time was compared to the best existing algorithms in the literature. Simulation results show the effectiveness of the proposed approach.

Keywords: energy cost; energy efficient path; Energy Internet; energy router; energy routing; P2P distributed energy trading; power loss; subscriber matching; transmission scheduling

Citation: Hebal, S.; Mechta, D.; Harous, S.; Dhriyyef, M. Hybrid Energy Routing Approach for Energy Internet. *Energies* **2021**, *14*, 2579. https://doi.org/10.3390/en14092579

Academic Editor: Branislav Hredzak

Received: 29 March 2021
Accepted: 26 April 2021
Published: 30 April 2021

1. Introduction

Due to the increase in energy demand and price, the environmental pollution resulting from conventional energy production techniques based on fossil fuel (coil, crud oil and natural gas), the development of environmentally friendly energy known as renewable energy, such as solar, wind and tide, has become necessary and attracted a lot of attention. The integration of renewable energy in the energy system reduces the CO_2 emissions, the transmission costs of energy and the load placed on the main grid by supplying a percentage of the demand through local energy production and consumption. Transforming energy production from conventional techniques to fully rely on renewable energy sources in the energy network cannot completely guarantee energy self-balancing due to its dispersion, discontinuity and volatility properties. The generation of energy, by these renewable sources, depends on weather conditions. Thus, renewable energy sources must be connected with the utility grid and controlled using sensing capabilities with information and communication technologies which creates smart grids [1]. According to National

Institute of Standards and Technology (NIST), USA, the smart grid (SG) is: "A modernized grid that enables bidirectional flows of energy and uses two-way communication and control capabilities that will lead to an array of new functionalities and applications". While SG uses an intelligent and digitized network, some restrictions still remain. In the aim of developing and completing the issues of smart grids, the EI was proposed [2,3]. The concept of EI, also called the Internet of energy and future smart grid, was proposed for the first time by the American economist Jeremy Rifkin in his book "The Third Industrial Revolution: How Lateral Power Is Transforming Energy, the Economy, and the World" [4], to solve the problems of existing energy systems. Jeremy Rifkin defined the EI as an energy system combined with the Internet technology in the aim of making an effective use of renewable energy, increasing the energy efficiency and the reliability of the electrical power system. EI is a complex energy system in which different energy networks are connected, such as: power grids, cooling/heating systems, natural gas networks, distributed energy generation, storage systems and loads [3]. The principle of EI is based on the integration of Internet technology, renewable energy, advanced technologies such as smart monitoring, intelligent management and large data processing with the existing energy systems [5,6]. The main objective of EI is to create a sustainable energy system with high energy efficiency, significant cost saving, minimum power losses and the high improvement of the use of distributed renewable energy sources (DREs).

As we mentioned before, the EI supports several forms of energy. In this paper, the energy flow is stored and distributed in the form of electrical energy.

In the conventional electrical power system, the power flow is unidirectional, generated by large scale power plant, transmitted to substations via high-voltage transmission lines and distributed to end users through low-voltage distribution lines. Accordingly, the power market is often structured in a unidirectional form, where generation companies generally sell huge amounts of electric energy to wholesale retailers, while retailers sell the electric energy to end users in smaller amounts [7,8]. With the concept of feed-in-tariffs (FiTs) in SG, consumers equipped with distributed renewable energy sources (DREs) referred to as prosumers—they can generate and consume electricity—are able to directly contribute in the power market by selling their excess energy to the utility grid (company) [9]. Many studies have been proposed in this regard to insure the supply–demand balance in the SG and to maximize the profit of the power market. Authors in [10] proposed a Stackelberg game-theoretic approach between the utility company and various prosumers, in which the utility company acts as a leader and announces an energy price, while the prosumers act as followers and adjust their electricity consumption according to the announced price. However, the authors in [11] proposed a contract-theoritic demand response management approach that aims to maximize the profit of both utility grid and prosumers in the SG. Unfortunately, the benefit of the involved prosumers in the FiT systems has been limited, prompting researchers to determine other trading schemes to encourage prosumers to become involved in power trading [12]. In contrast, EI is a peer-to-peer energy sharing system with a bidirectional flow of power and communication. The emergence of P2P distributed energy trading (sharing) in EI provides a new public energy market with new features in the power system. It enables prosumers to trade and share their excess energy (power) with each other directly in peer-to-peer mode without the interaction of a central entity such as a utility company [13]. This peer-to-peer mode of energy exchange gives energy producers and consumers the opportunity to create some financial benefits by selling the excess energy (generally with a lower cost than the cost of a utility company) instead of storing it for future use, which creates some power losses. Additionally, it decreases the consumer's electricity bills and the reliance on the main grid (utility company). As far as we know, due to its complex technologies and infrastructures, there is no standardized architectural model for P2P electrical energy trading and various types of P2P distributed energy trading architectures have been designed by various studies [14–17].

The expansion of the use of DREs in power generation with their volatility, the transformation of the generation and the injection of power from centralized to distributed manner, the peer-to-peer energy sharing and the power losses during the energy transmission process make the distribution of energy and the balancing of energy supply/demand in EI more difficult. All of these variables gave rise to the key issue of the Energy Internet, which is the energy routing issue. It is known that there is some power losses during energy transmission process between producers and consumers. In order to minimize the power losses and to create efficient energy delivery over the EI, energy routing has been suggested which was inspired by data routing on the Internet. Energy routing is the process that facilitates the transmission of energy between prosumers and consumers situated in different geographic locations with the minimum power transmission losses. The key element of EI and energy routing is the energy router (ER), which is used to route both information and energy flow [18,19]. Current energy systems do not have this capability. However, energy routing in distributed energy systems is more complicated due to integration problems; because power conversion from one type to another may be needed. Energy routing has received considerable attention from the research community in recent years. Current research on this issue includes designing energy routing devices and energy routing algorithms. A number of researchers considered energy routing as data routing and therefore suggested devices and protocols for energy routing. Nonetheless, energy routing criteria are distinct from data routing (see Table 1). The waste packet can be resent in the Internet, which is not possible in EI. In addition, energy routing is demand-driven and the source of the energy is not defined [13]. Furthermore, an energy overflow may cause system devices or even the whole system to crash. Therefore, energy routing has more requirements on safety and reliability than data routing. For that, energy routing protocols are the main field of research for working on EI. These energy routing algorithms need to solve three main problems: the subscriber matching problem by determining the best producer for each consumer; the efficient energy routing problem by selecting the best path with the minimum power loss between these producer–consumer pairs; and finally, scheduling these energy transmissions to prevent congestion or overflow problems.

Table 1. A comparison in routing design between the Internet and Energy Internet.

Category of Comparison	**Internet**	**Energy Internet**
Transmission	Data (Information)	Energy (electricity)
Transmission lines	Wired and wireless connections	Power lines (grid)
Routing devices	Network routers and switches	Energy routers and smart meters
Transmission loss	No losses	Loss exist
Objective of routing	Efficient data transmission	Efficient energy transmission Minimize the power losses
Challenges	Shortest transmission path Congestion management	Subscriber matching Energy Efficient transmission path Transmission scheduling
Criteria (characteristics)	Demand dominated The source of data packet is predefined Regenerate the waste packet	Demand dominated The source of energy is not defined Cannot regenerate the wasted energy

Current literature indicates that the different energy routing algorithms proposed to solve the energy routing are usually based on graph theory, game theory, mixed integer programming and autonomous systems. In the graph theory-based routing algorithms, the grid is presented as a graph and routing methods are applied to find the lowest cost path such as: the protocol proposed by Wang et all in paper [20]. In this work, the proposed energy routing protocol finds all the possible paths between the consumer and producer in the grid, and then determines the best path among them. This solution is not practical, especially in large grids, as the proposed protocol assumes that the transmission capacity of transmission lines is large enough. In paper [21], the authors proposed a distributed routing algorithm based on Dijkstra algorithm. This study did not investigate how the prosumer–consumer pairs are created. The authors in [22] proposed a hierarchical energy routing protocol where a master node determines all efficient paths between each pair in the grid, which affects the security and efficiency of the grid, and could cause the one point failure of the system. However, game theory has been widely used in power systems to solve different issues such as the demand response optimization problem including the work in [23] where a Stackelberg game approach was proposed in order to reduce the peak load and balance the supply–demand in the smart grid. The proposed approach determines the efficient consumption scheduling for consumers based on the real-time pricing. The authors in [24] used the reinforcement learning with the game theory and proposed an approach to solve the demand response problem in SG—in which a reinforcement learning mechanism was used to determine the best company for each consumer based on the electricity price and availability, and game theory based-demand response management technique to schedule the consumer consumption. Several game theory based-approaches [25–28] have been proposed to solve the energy routing problem in the peer-to-peer energy trading market. In these approaches, producers and consumers play a game (such us Stackelberg game, Coalition game . . . etc.) to create the producer/prosumer–consumer pairs with the maximization of their benefits. An energy routing algorithm based on an autonomous system is proposed in [29] where each system entity acts as an agent in the trading process. Authors in [30] proposed an energy trading platform with a mixed integer programming model for the optimal sharing energy between different houses in the EI in order to create a total profit for all participant houses. This work introduced a decision-making process that allows houses to determine when they should buy or sell energy, but it did not investigate the efficient path and scheduling problems. However, the authors in [31] suggested the use of bio-inspired methods to solve the energy routing problem. They considered the energy routing problem as an optimization problem and proposed the use of Ant Colony Optimization (ACO) to solve it. The proposed protocol calculates the minimum loss path between producers and consumers using the distance with the average cost by mile. A distributed Bee Colony Optimization (BCO)-based energy routing protocol is proposed in [32] to determine the best producer for each consumer considering the power loss, distance and available power among producers. The authors in [33] proposed an optimized energy routing method using Particle Swarm Optimization (PSO). It determined the energy-efficient path between producers and consumers in the SG by considering the links' quality, transmission cost and latency in the selection of the best optimal neighbors. There are other considerations than distance to be included in the estimation of the power loss, which will be addressed in detail in the next section. Based on the previous analysis, we considered in this paper the energy routing problem with its surrounding issues (subscriber matching, efficient path and transmission scheduling) as an optimization problem. To solve this problem, we proposed an improvement of the existing energy routing method in [31]. The contributions of this paper are:

- A peer-to-peer energy trading architecture based on energy routers;
- A subscriber matching mechanism, and an Energy Particle Swarm Optimization Algorithm (*EPSOA*). The proposed subscriber matching mechanism determines the consumer–producer pairs for both mono and multi-source consumer cases (normal and heavy loads). The *EPSOA* is used in a heavy load case to determine the amount power to buy from a set of producers to insure minimum power transmission loss and cost;
- An Improved energy routing protocol based on ant colony optimization which calculates a non-congestion minimum loss path between each producer/consumer pair in the EI.

The remaining sections of the paper are organized as follows. Section 2 describes the proposed EI based on energy routers. It is modeled as a weighted graph. Section 3 introduces the subscriber matching mechanism, the energy particle swarm optimization method with the centralized peer-to-peer energy trading network. The Improved Ant Colony Optimization (IACO)-based energy routing protocol is detailed in Section 4. The performance of the proposed algorithms is evaluated by various analysis cases. It is also compared to the algorithm described in Section 5 in terms of power losses, costs and computation time. Finally, Section 7 concludes the paper.

2. Implementation of Energy Internet with Energy Routers

In this section, the structure of ER-based energy Internet and its graph theory representation are introduced. The concept and functions of ER are discussed.

2.1. Structure of Energy Internet with Energy Routers:

As illustrated in Figure 1, the proposed energy router-based EI in this paper consists of different passive consumers (e.g., smart homes, industrial users, buildings, EVs), distributed power generation units such as solar and wind power, distributed energy storage units, and active consumers referred to as prosumers. As mentioned earlier, a prosumer is a consumer equipped with DREs (such as solar panels, wind turbines) to generate and consume electricity. In this work, the prosumer is represented by a smart home equipped with solar panels, such as in [34]. In the SG, prosumers trade their surplus energy with the utility grid for a small feed-in-tariff rate, which is not the only trading option in the EI. As mentioned earlier, the EI is a peer-to-peer energy sharing system that enables passive consumers equipped with distributed energy sources to trade directly and share energy with each other without the interaction of the utility grid. This creates some benefits for prosumers, consumers and the utility grid. All these elements are connected to a net structure using power lines and energy routers.

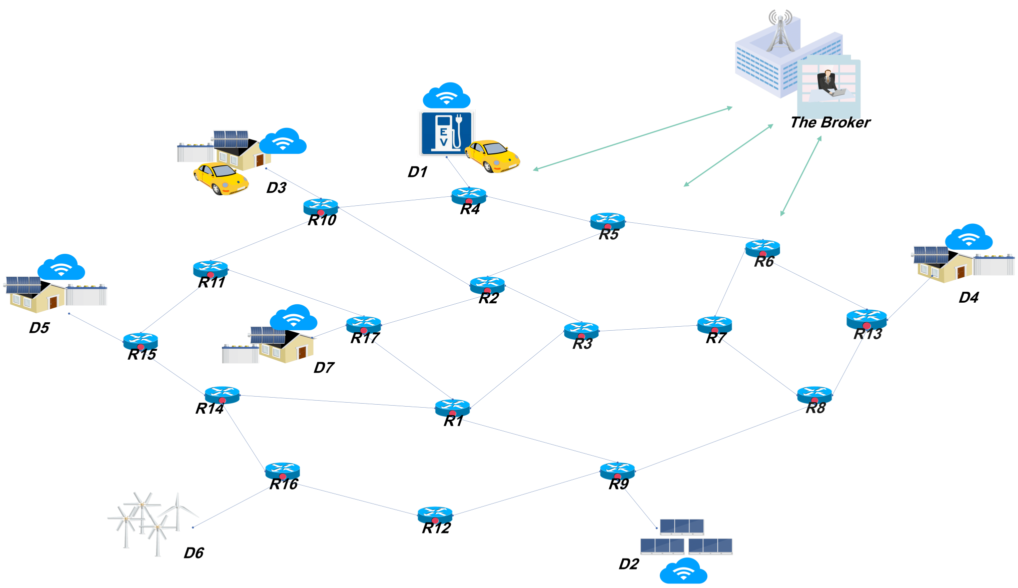

Figure 1. Example structure of the proposed Energy Internet.

In our system, we consider that the grid used is a three-phase electrical grid characterized by the composed voltage $V = 400$ v, and the frequency of 50 Hz. The apparent power requested by the consumer is:

$$S_{Apparent} = \sqrt{P^2 + Q^2} \tag{1}$$

where P represents the active power ($P = \sqrt{3} \times V \times I \times cos(\phi)$) and Q is the reactive power ($Q = \sqrt{3} \times V \times I \times sin(\phi)$) with $I, cos(\phi)$ represents the line current and the power factor, respectively. In general $cos(\phi) > 0.95$, and as a result, the reactive power becomes negligible, and the apparent power is approximately equal to the active power ($S_{Apparent} \simeq P$).

The producer produces power that is an active power since the energy router (converters) do not inject reactive power into the grid.

In the aim of creating an efficient, scheduled, stable and controlled peer-to-peer energy trading market, we propose a centralized peer-to-peer energy trading architecture that contains a principal actor, named the broker. This broker manages the energy market and adjusts to balance the supply and demand in the energy system by satisfying consumers requests without the need of adding new energy generation units. The broker's role will be discussed in detail in the following section.

Using graph theory, the proposed EI is modeled as a weighted graph $G = \{V, E, W\}$ as shown in Figure 2.

- Energy routers are represented by a set of vertices $V = \{v_1, v_2, \ldots, v_n\}$;
- Power lines used for connecting energy routers are represented by a set of edges $E = \{e_{ij}, \ldots\}$, where e_{ij} is the power line that connects router v_i to router v_j;
- W describes the adjacency matrix of the network $W = (w_{ij})_{n \times n}$, which reflects the network topology with the weights of both ERs and power lines of EI as shown in Equation (2).

$$w_{ij} = \begin{cases} w_{e_{ij}} & e_{ij} \in E \\ w_{v_i} & i = j \\ \infty & e_{ij} \notin E \end{cases} \tag{2}$$

where $w_{e_{ij}}$ is the weight of the edge e_{ij}, which represents the power loss of the power line that connects routers v_i and v_j. While w_{v_i} is the weight of ER v_i, which represents its power loss. Both weights of power lines and energy routers are determined by Equations (15), (18) and (19) as shown in Section 5.

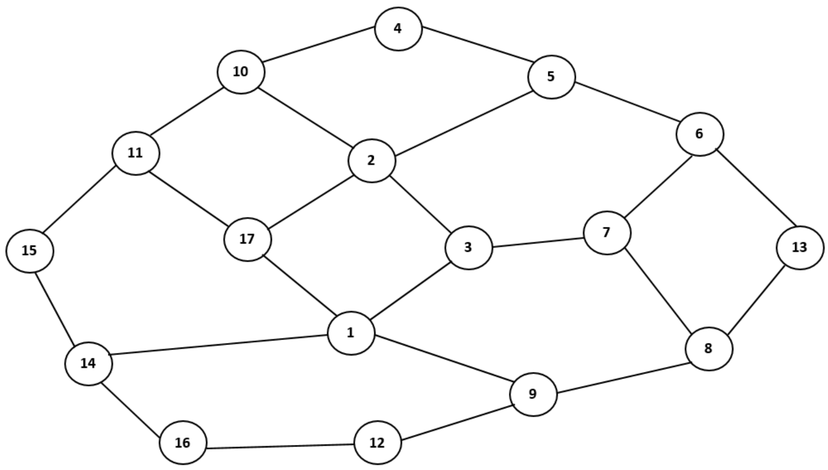

Figure 2. Energy Internet model.

2.2. Energy Router Architecture and Functions

ER is regarded as the primary networking unit for the implementation of the EI. It is proposed to achieve a better utilization of renewable energy sources, with an efficient transmission of energy flows. The ER has comprehensive functions such as an energy exchange, communication and energy management [35]. The study of ERs is in its preliminary stage at present, and various researchers have suggested different ER designs, such as the works in [20,35–37]. The common functionalities between the different suggested designs are: the integration of renewable energy sources; the control of power and communication flows; and the regulation of power quality and voltage/frequency conversion.

The first design of ER was based on solid-state transformers (SSTs) and proposed by The Future Renewable Electric Energy Delivery and Management (FREEDM) [38]. As shown in Figure 3, the SST-based ER is composed of an energy management module and power electronic conversion module SST [6,37]. First, the energy management modules can realize the communication, power routing and management using power flow, while the power electronic conversion module (SST) can convert multiple energy forms and voltage levels, as well as compensate for reactive power. It has a three-stage topology: the high-voltage AC/DC stage, the middle DC/DC stage and the low-voltage DC/AC inverter stage. The high-voltage AC/DC stage rectifies the power frequency from High Voltage Alternating Current (HVAC) to Medium Voltage Direct Current (MVDC), the bidirectional middle DC/DC stage transforms the the MVDC to a regulated Low Voltage Direct Current (LVDC), while the low-voltage DC/AC inverters generate a LVAC. The SST provides multiple plug-and-play interfaces that allow loads, storage systems, renewable energy, micro-grids (MGs), utility grid and other ERs to be connected. Every interface can connect various energy systems or devices, provided that the total power connected to the interface does not surpass its capacity limits.

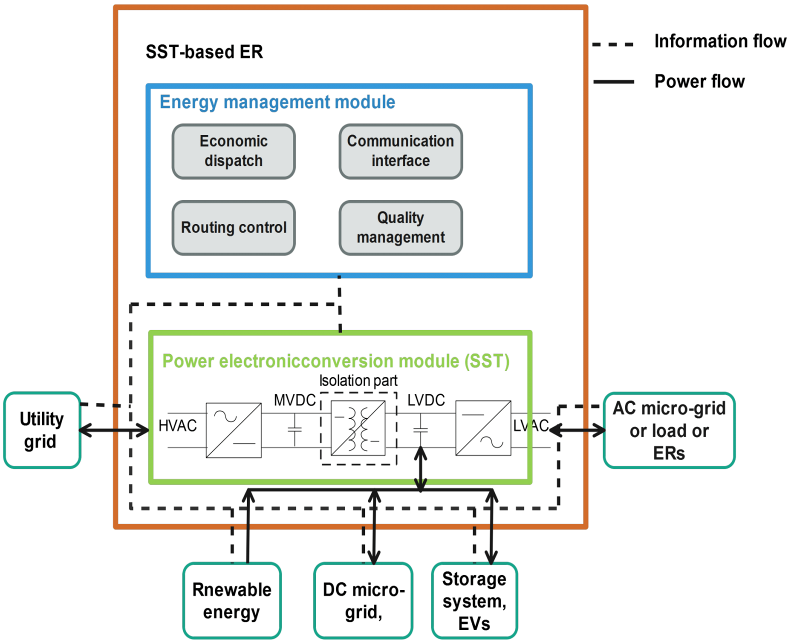

Figure 3. SST-based ER architecture.

Using ER controlled by information can improve the efficiency of energy transmission and energy allocation. For an efficient energy management, these ERs need to be equipped with efficient dynamic energy routing protocols to respond to changes in energy information, system topology and the regular connection/disconnection of the system devices. For this, in our proposed network architecture, we assume that every ER broadcasts its energy information, its connections (ERs, devices and power links) with their energy information to all other ERs in the system. Whenever the system topology or energy information change, the connected ER broadcasts this information to all the others. Thus, each ER accumulates all the necessary energy information and topology of power system and stores them in two different energy information tables, as shown in Tables 2 and 3. These tables represent the energy information of the proposed EI in Figure 1 where eff represents the power conversion efficiency of the corresponding ER converter.

Table 2. Energy information of ERs.

ER	Interface Capacity (kw)	Conversion Efficiency (*eff*)
R_1	20	1
R_2	15	0.98
R_3	25	1
R_4	24	1
R_5	22	0.98
R_6	20	0.97
R_7	25	0.98
R_8	30	0.97
R_9	30	1
R_{10}	20	0.97
R_{11}	27	1
R_{12}	25	0.98
R_{13}	30	1
R_{14}	19	0.98
R_{15}	18	1
R_{16}	18	0.97
R_{17}	20	0.98

Table 3. Energy information of power lines connecting ERs.

Power Line	Capacity P^C_{line} (kw)	Resistance (Ω)	Voltage (V)
L_{1-3}	30	0.6	400
L_{1-9}	45	0.45	400
L_{1-14}	40	0.21	400
L_{1-17}	30	0.24	400
L_{2-3}	20	0.64	400
L_{2-5}	20	0.51	400
L_{2-10}	30	0.19	400
L_{2-17}	30	0.19	400
L_{3-7}	45	0.94	400
L_{4-5}	24	0.19	400
L_{4-10}	30	0.64	400
L_{5-6}	7	0.45	400
L_{6-7}	40	0.24	400
L_{6-13}	30	0.21	400
L_{7-8}	10	0.21	400
L_{8-9}	32	0.65	400
L_{8-13}	40	0.19	400
L_{9-12}	32	0.45	400
L_{10-11}	30	0.24	400
L_{11-15}	32	0.6	400
L_{11-17}	40	0.24	400
L_{12-16}	40	0.21	400
L_{14-15}	30	0.45	400
L_{14-16}	35	0.19	400

3. Energy Routing Approach

Due to the structure and characteristics of EI, some features must be considered in the routing approach:

- Energy routing is demand-dominated and the source of energy is not specified;
- The lost energy cannot be regenerated and may cause an overflow that could lead to the destruction of devices/lines, or even the crash of the whole energy system;
- The power transmission loss is not only related to the length of the path but also to the transmitted and pre-existing power. Because of this fact, the ERs should not store the routing paths but the energy information of the whole system;
- The dynamic routing algorithm must achieve the supply–demand balance.

Taking into account these features, we considered the energy routing problem as an optimization problem, where the objective function is to minimize the power transmission losses and cost. To solve this issue, we proposed:

- A centralized peer-to-peer energy trading architecture;
- A subscriber matching mechanism for both mono and multi-source consumer cases. This mechanism assigns for each consumer the optimal producer in terms of minimization of both cost and power loss;
- In the case of multi-source consumer (heavy load), we proposed an energy particle swarm optimization algorithm, to determine the amount of power for a set of producers to achieve minimum power transmission loss and cost;
- An IACO-based energy routing protocol that ensures a non-congestion efficient-energy transmission.

4. Subscriber Matching Mechanism

The subscriber matching mechanism constructs the producer (seller)–consumer (buyer) pairs based on the proposed peer-to-peer trading architecture. We assume that, here, the broker stores producers/consumers profiles such as: the electricity price, transmission time and the amount (P) of available/needed power, as shown in Table 4.

Table 4. Producers' and consumers' energy information.

Device	Consumer/ Prosumer	P (Kw)	Electricity Price (USD/Kw.h)	Transmission Time (h:m)
D1	Consumer	−22	-	13:00–13:15
D2	Prosumer	15	0.068	09:45–14:00
D3	Consumer	−9	-	10:00–12:00
D4	Prosumer	25	0.048	09:00–12:00
D5	Prosumer	10	0.056	12:00–13:30
D6	Prosumer	18	0.043	12:30–14:00
D7	Consumer	−12	-	10:00–12:00

As mentioned in the subscriber-matching mechanism sequence diagram (shown in Figure 4):

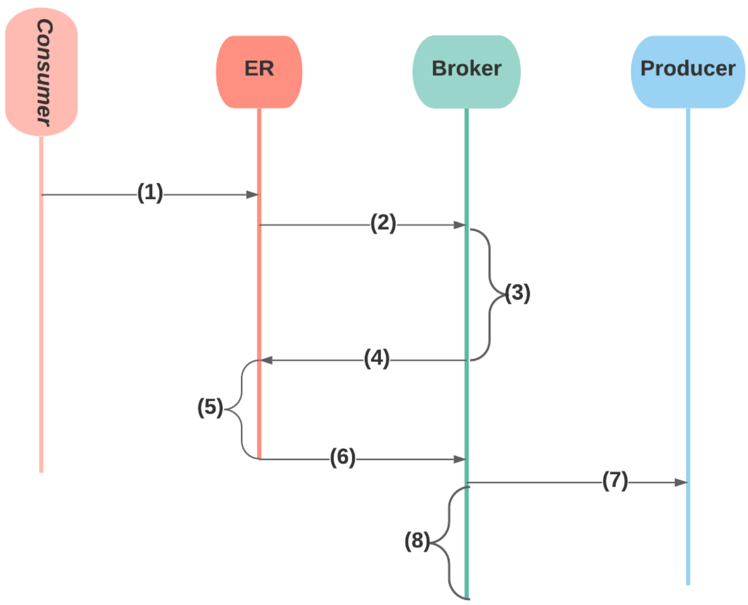

Figure 4. Energy routing approach sequence diagram.

(1) Each consumer creates an energy request message with the amount of needed energy, then sends it to their connected ER.
(2) The ER transfers this energy request to the broker.
(3) The broker treats the energy demands according to their requesting time and determines for each demand a list of all producers/prosumers that can provide the consumer energy demand in the corresponding time. If there is no single producer/prosumer capable of providing the consumer required energy, then the consumer is a heavy load. In this case, the broker constructs a list of all the producers/prosumers available in the consumer transmission time;.
(4) The broker sends the constructed list to the consumer energy router.
(5) After receiving the possible producers' list, the consumer ER runs the subscriber matching mechanism as illustrated in Algorithm 1,

As illustrated in Algorithm 1, there are two cases:

Algorithm 1: Subscriber Matching Mechanism

```
Input: c                                        // the identify of consumer
       P_c                                      // the demand energy of consumer
       L                                        // the list of possible producers
Output: Fitness                                 // the Fitness value
/* check if the consumer is a heavy load                                  */
Fitness ← 0
if !heavyLoad(c) then
    /* case 1: Mono-source consumer                                       */
    for i ← 0 to l do
                                      // l:the number of producers in list L
        cost_p ← calculatecost(L(i), P_c)
        w_{c↔p} ← IACObasedERP(L(i), c, P_c)
        Fitness_p(i) ← α × w_{c↔p} + (1 − α) × Cost_p
    /* Select the best producer with min Fitness                          */
    Fitness = min(Fitness_p)
else
    /* case 2: Heavy load (consumer)                                      */
    C_n^c ← createCombination(P_c, L)
    for i ← 1 to m do
        /* Determine the power amount to get from each set to achieve the minimum
           Fitness                                                        */
        Fitness_s(i) ← EPSOA(C_c^n(i), c, P_c)
    /* Select the best producers set with the min Fitness                 */
    Fitness ← min(Fitness_s)
```

Case 1: A mono-source consumer

Here, one or multiple producers can provide the requested energy. Here, ER uses Equation (3) to calculate the fitness value ($Fitness_p$) to each producer (p) in the received list.

$$Fitness_p = \alpha \times w_{c \leftrightarrow p} + (1 - \alpha) \times Cost_p \tag{3}$$

$$Cost_p = electricityPrice \times P_c \times Time \tag{4}$$

where $cost_p$ and $w_{c \leftrightarrow p}$ represent, respectively, the cost of energy and the power transmission loss of the best path between the consumer and producer generated by IACO-based energy routing protocol (described in detail in Section 5).

As mentioned in Equation (3), it is evident that the objective function combines two opposing objectives to be minimized: cost and power loss. To make the problem simpler, we connected these two objectives together by an α factor reflecting the degree of importance or weight of each objective, based on the preference of the broker. Thus, for instance, if the broker wants to reduce the $Cost_p$ by giving 80% of importance to the $Cost_p$, the importance of the power loss $w_{c\leftrightarrow p}$ will be just 20% and α in this case is equal to 0.2. If the broker wants to give the same importance to the two objectives, α took the value 0.5.

The broker decides the value of α according to the system generation capacities. Whenever the number of producers or power generation capacity decreases, the degree of power loss importance increases.

(6) The ER selects the producer with the minimum fitness value (Equation (5)), informs the broker to do the necessary updates (8) and to inform the selected producer (7), creates the virtual circuit to start the transfer of energy using the selected efficient path, updates the pre-existing power in its power tables and informs the other ERs:

$$Minimize\left(Fitness_p\right) \tag{5}$$

Case 2: A multi-source consumer (heavy load)

In this case, none of the available prosumers can provide the whole demanded energy, so multiple producers would be chosen by the subscriber matching mechanism to satisfy the consumer demand. The number of selected suppliers for a given consumer (load) should be as limited as possible, to minimize the subscriber matching mechanism complexity, maximize the stability and ensure the security and robustness of the grid [20,21,39]. Using the possible producers list (L), first, the ER creates a vector C_n^c of a set of producers/prosumers.

$$C_n^c = \begin{pmatrix} S_1 \\ S_2 \\ \cdots \\ S_m \end{pmatrix}_{m\times 1} = \begin{pmatrix} p_{11} & p_{12} & \cdots & p_{1n} \\ p_{21} & p_{22} & \cdots & p_{2n} \\ \cdots & \cdots & \cdots & \cdots \\ p_{m1} & p_{m2} & \cdots & p_{mn} \end{pmatrix}_{m\times n}$$

Each set S in C_n^c contains a number of producers (n), where the sum of their available power satisfies the consumer's demand (6):

$$\Sigma_{k=1}^{n} P_k >= P_c, k \in L \tag{6}$$

Then, for each set S_k in C_n^c, the ER invokes the energy particle swarm optimization algorithm ($EPSOA$) to determine the required power amount from each producer in set S_k to obtain the minimum fitness value ($Fitness_{S_k}$):

$$Fitness_{S_k} = \Sigma_{i=1}^{n} Fitness_{p_i} \tag{7}$$

Algorithms 2 and 3 represent the proposed energy particle swarm optimization algorithm ($EPSOA$) with its objective function, respectively. The algorithms' parameters are shown in Table 5.

The $EPSOA$ initially creates k particles. A particle reflects the amount of power to be supplied by each producer in the set S to satisfy the consumer demand (each particle is equivalent to one row in the energy combination matrix). In each particle, if the set contains n producers, the amount of power obtained from producer 1 to producer $(n-1)$ is randomly within the permissible range, while nth producer completes the consumer demand. The algorithm evaluates the fitness value including cost and power loss (Equation (7)) of each particle using the objective function in Algorithm 3, initializes $pbest$ and chooses the particle with the minimum fitness value as $gbest$. The algorithm is iterative where in each iteration, the values of X and V are updated using Equations (7) and (8). These equations are taken from [33].

$$V_i^{t+1} = wV_i^t + C_1r_1[pbest_i^t - X_i^t] + C_2r_2[gbest^t - X_i^t] \tag{8}$$

$$X_i^{t+1} = X_i^t + V_i^{t+1} \tag{9}$$

The new values of X^{t+1} must verify the constraints (10), (11), (13) and (14) while the values of *pbest* and *gbest* are updated as in Algorithm 2.

Algorithm 2: Energy Particle Swarm Optimization

```
Input: c, P_c, S
Output: f0min, gbest
Initialize the PSO parameters (k, n, C_1, C_2, and w)
                         /* Initialize the random positions of each particle (X_i) */
i ← 1
while i <= k do
    for j ← 1 to n do
        X(i,j) ← Rand(X(i,j)_min, X(i,j)_max)
    if X(i,m)_max <= P_c − sum(X(i,n−1)) then
        X(i,j) ← P_c − sum(X(i,n−1))
        i ← i+1
        Initialize the particle velocity V(i)
                         /* Evaluate the fitness function of each particle */
for each particle i do
    f_0(i) ← OF(X(i,:), S, c)
[f0min, index] ← min(f_0)
pbest ← X
gbest ← X(index)
ite ← 1
while (ite <= maxit) && !(error criteria) do
    Update V according to Equation (8)
    for each particle i do
        for each producer j in S do
            Update X according to Equation (9)
            X(i,j) ← X(i,j) + V(i,j)
        f(i) ← OF(X(i,:), S, c)
        if f(i) < f_0(i) then
            f_0(i) ← f(i)
            pbest(i) ← X(i,:)
    [fmin, index] ← min(f_0)
    if fmin < f0min then
        gbest ← pbest(index)
        f0min ← fmin
    i ← i+1
```

Algorithm 3: *EPSOA* Objective Function (OF)

Input: X, S, c
Output: $Cost$
Function `OF`(X, S, c)**:**
    $Fitness \leftarrow 0$
    for $i \leftarrow 1$ **to** n **do**
        $cost_{S(i)} \leftarrow calculatecost(S(i), X(i))$
        $w_{c \leftrightarrow S(i)} \leftarrow IACObasedERP(S(i), c, X(i))$
        $Fitness \leftarrow Fitness + \alpha \times w_{c \leftrightarrow S(i)} + (1 - \alpha) \times Cost_{S(i)}$
    end
    return $Fitness$
End Function

Table 5. Algorithm 2's parameters.

Symbol	Description
c	The consumer
P_c	The amount of consumer demand energy
S	Set producers from the C_n^c
$S(i)$	The ith producer of set S
k	The population size (number of particles)
n	The number of consumers in set S
C_1, C_2	Positive acceleration constants
r_1, r_2	Random values ($0 \leq r_1, r_2 \leq 1$)
w	Inertia factor
X	The position of the particles which represents the amount of energy to took from each producer in the set S, $X(i) = [P_1 \dots P_m]$
$X(i,j)_{min}$	The minimum amount of energy that could be provided by producer j in set S_i. (in our case 0)
$X(i,j)_{max}$	The maximum amount of energy that could be provided by producer j in set S_i (P_j)
V	The velocity
f_0	The fitness value of the initial X (the energy transmission cost of the corresponding energy in X)
f	The fitness value of X (the energy transmission cost of the corresponding energy in X)
$pbest$	The personal best solution of each particle which represents the best amount of energy to get from each producer in set S to reach the consumer demand with minimum transmission cost
$gbest$	The global best solution, which represents the best particle (energy amount) with the minimum fitness
$maxit$	The max iterations number

- The total amount of power in the particle must be equal to the consumer demand:

$$\Sigma_{i=1}^{n} X_i = P_c \tag{10}$$

- The amount of power from producer j in particle i must be within the producer's capacity (the available power):

$$0 < X_{ij} \leq P_{p_j} \tag{11}$$

Finally, after the determination of the required power amount from each producer in each set with the minimum energy transmission cost, the ER selects the best set using Equation (12):

$$Fitness_{min} = min_{k=1\dots m}(Fitness_{S_k}) \tag{12}$$

The ER obtains the best set with all the necessary information (required power, best path to each producer in the best set) and as in case 1, it creates the circuit, does the necessary updates and informs the broker, and then starts the energy transmission from selected producers.

The consumer–prosumer pairs, produced by the subscriber matching, should satisfy the following constraints:

- If the prosumer/producer is matched with multiple consumers, the total amount of selling electricity (p_{cp}) should not exceed the existing power of the prosumer (P_p):

$$0 \leq \Sigma_{c=1}^{k} p_{cp} \leq P_p \tag{13}$$

- If the consumer is matched with multiple prosumers, the total amount of buying electricity (p_{cp}) should not exceed the demand energy of the consumer (P_c):

$$0 \leq \Sigma_{p=1}^{k} p_{cp} \leq P_c \tag{14}$$

5. Improved ACO-Based Energy Routing Protocol (IACO-ERP)

Each ER connected to a consumer executes an IACO-based energy routing algorithm to determine the energy-efficient path between each producer–consumer pair.

In this work, we selected the energy transmission path depending on its power transmission loss. The power transmission loss of a path is related to two main factors: the power lines losses (w_{ij}) and ER losses (w_i) that construct the path. w_{ij} and w_i represent the weights of ERs and power lines in the EI model shown in Figure 2.

The power loss in ER is dependent on the conversion efficiency of the electronic converters and the power cable transmission losses inside it. Since the latter is neglected and the conversion efficiency is assumed to be constant, the power loss of ER is a linear function of transmitted power (15). Where we have eff_i, P_{cp} represents the conversion efficiency of router v_i and the transmitted power from producer to consumer, respectively:

$$w_i = (1 - eff_i) \times P_{cp} \tag{15}$$

On the other hand, the total power loss in a power line between energy routers v_i and v_j is calculated based on the resistance (R_{ij}) and reactance (X_{ij}) of the line. Since a three-phase grid is used, it was noted that the total power loss of the line is divided into active and reactive power losses:

$$w_{ij} = \sqrt{P^2_{activepowerloss} + Q^2_{reactivepowerloss}} \tag{16}$$

with $P_{activepowerloss} = 3 \times R_{ij} \times I^2$ and $Q_{reactivepowerloss} = 3 \times X_{ij} \times I^2$. It is known that the reactive power loss is negligible compared to the active power loss and the total power loss in the line becomes:

$$w_{ij} = 3 \times R_{ij} \times I^2 \tag{17}$$

Equation (18) describes the relation between the line power loss and the transmitted power:

$$w_{ij} = \frac{R_{ij}}{V_{ij}^2} \times P_{cp}^2 \tag{18}$$

where R_{ij} and V_{ij} are the resistance and voltage of the power line that connect energy routers v_i and v_j, respectively. However, P_{cp} is the transmitted power of consumer–producer pair. In fact, Equation (18) is not relevant in the case where there is an already existing power (P_{ij}) in the line. In this case, the power line loss is calculated using Equation (19):

$$w_{ij} = \frac{R_{ij}}{V_{ij}^2} \times \left[\left(P_{cp} + P_{ij}\right)^2 - P_{ij}^2 \right] \tag{19}$$

Accordingly, the total power loss of a transmission path that connects a consumer–prosumer pair is the sum of power losses of all routers and power lines that construct the path.

$$w_{c\leftrightarrow p}^{path} = \Sigma_{v_i \in path} w_i + \Sigma_{e_{ij} \in path} w_{ij} \tag{20}$$

To select the minimum loss path between consumer–prosumer pairs, we proposed an improvement of the protocol in [31]. We introduced an improved ACO-based energy routing protocol IACO-ERP, which allows the selection of a non-congestion efficient path, where the objective function is the minimization of the power transmission loss (Equation (21)):

$$w_{c\leftrightarrow p} = min\left(\Sigma_{k \in paths} w_{c\leftrightarrow p}^{k}\right) \tag{21}$$

The flowchart in Figure 5 describes the fundamental concept and implementation of the IACO-based energy routing protocol used to find the non-congestion minimum loss path. The relevant parameters are shown in Table 6.

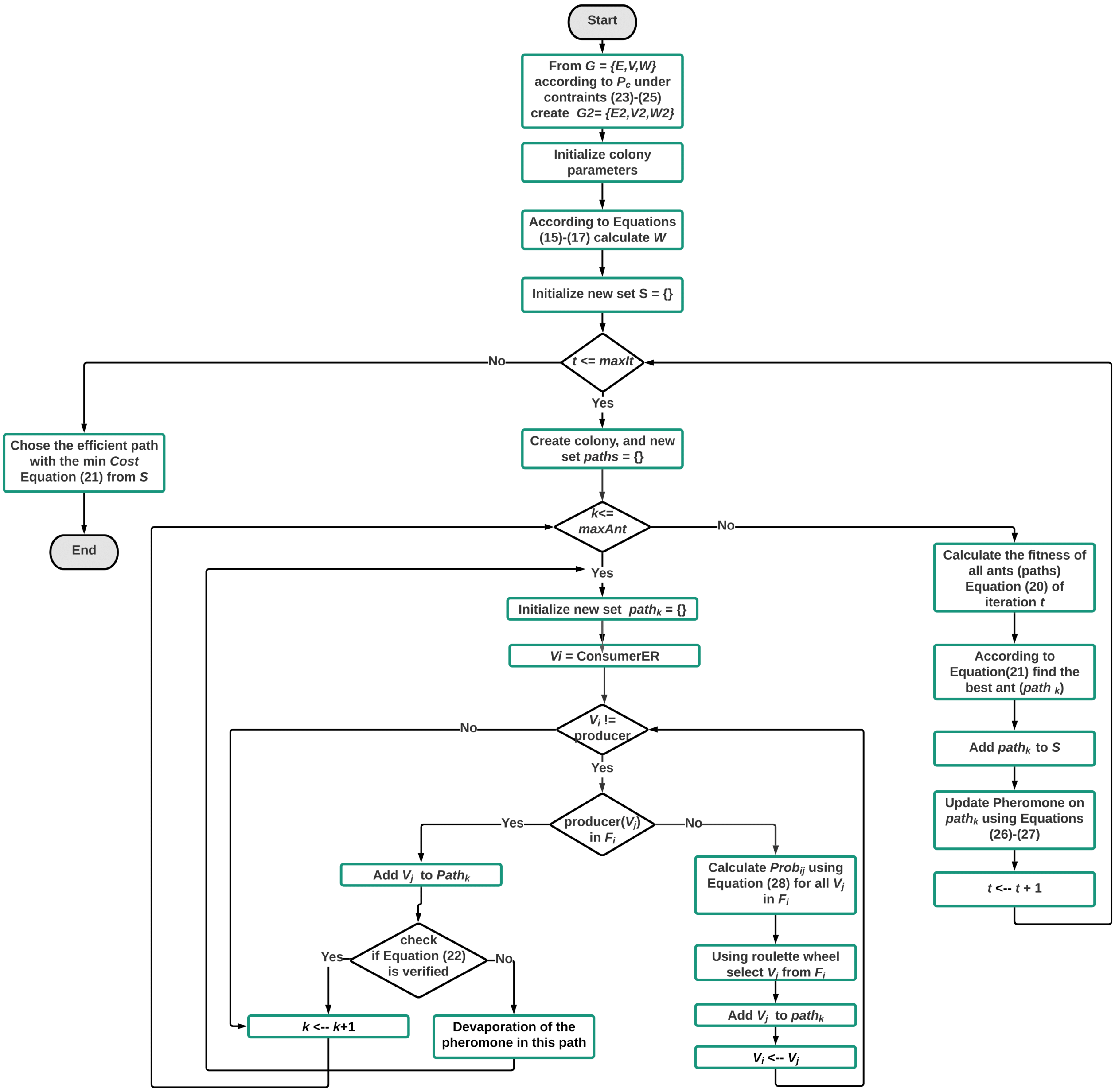

Figure 5. Improved ACO-based energy routing protocol (IACO-ERP).

Table 6. IACO-ERP's Parameters.

Symbol	Description
$G = \{E, V, W\}$	The Energy Internet-corresponding graph model, where E, V, W represents the set of nodes, edges that consist the graph G with their weights, respectively
$G2 = \{E2, V2, W2\}$	The new graph of EI that can support the transmission of p_{cp}
S	A set of the best paths of each iteration
$maxit$	Iterations maximum number
$maxAnt$	Ants maximum number
$paths$	A set of all paths determined by all ants in one iteration
$path_k$	An energy transmission path between the consumer–producer pair determined by an ant k
V_i	The current node where the ant is allocated
V_j	A neighbor of node V_i (the next node to producer)
F_i	A set of one hop neighbors of a node v_i

The energy minimum loss path should satisfy the following constraints:

- The power loss of a path should be less than the transmitted energy:

$$w_{c\leftrightarrow p}^{path} < P_{cp} \tag{22}$$

- The transmitted power should not exceed the maximum capacity of the path, which is the minimum between the lowest interface capacity of energy routers and the lowest capacity of the power lines that constructed the path:

$$P_{cp} \leq min\left(P_{c\leftrightarrow p}^{Lines\_c}, P_{c\leftrightarrow p}^{ERs\_c}\right) \tag{23}$$

- The total power transmitted through a power line should not exceed its available capacity:

$$\Sigma P_{(v_i,v_j)} \leq P_{(v_i,v_j)}^{c} \tag{24}$$

- The total power flows into the same ER interface should not exceed its interface capacity:

$$\Sigma P_{(v_i,v_j)} \leq P_{v_i}^{c} \tag{25}$$

The energy routing selection method, in Figure 5, consists of ten steps which are carried out for each consumer–producer pair:

1. First, ERs constructs the network model using the system information (Tables 2 and 3).
2. Thereafter, receiving the pair information (the amount of transmitted power P_{cp}, identity of the producer/prosumer) and using the constraints (23)–(25), the ER eliminates all edges and nodes(ERs) that cannot transfer the P_{cp} and deducts a sub-graph G2.
3. The path selection method is based on ACO. Consumers and producers/prosumers represent the ant nest and food source, respectively. Ants are used to determine the best path between them. They use a chemical known as pheromone to communicate and trace the path to the food source. The path with the highest intensity of pheromone is the one widely used by ants. It is usually the shortest path. In nature, some ants depose more pheromones in the case where the food source is big or of higher quality and the path is very good [40]. Therefore, the pheromone level of a path is proportional to its power transmission loss.
   The amount of deposed pheromone on an edge (power line) e_{ij} by ant k is represented by Equation (26):

$$\Delta t_{ij}^{k} = \frac{1}{w^{path}} \tag{26}$$

where w^{path} is the power transmission loss of the path where the line e_{ij} belongs to this path. When the line e_{ij} connecting routers v_i and v_j is chosen by an ant k, the amount of pheromone on this line is updated using Equation (27):

$$\tau_{ij}^{k} = \Sigma_{k=1}^{n} \Delta t_{ij}^{k} \tag{27}$$

where n represents the number of ants selected on the line e_{ij}.
In this step, the ER initializes the colony parameters: number of iterations, ants, and pheromone level.

4. Each ant travels from the graph from one node (ER) to another until it arrives to the producer. The selection of the next hop (node) is determined by calculating a probability for each neighbor with the use of the roulette wheel principle. The probability depends on the amount of pheromone and the power loss to the next hop:

$$Prob_{ij} = \frac{(\tau_{ij})^{\alpha} (\eta_{ij})^{\beta}}{\Sigma_{j \in F_i} (\tau_{ij})^{\alpha} (\eta_{ij})^{\beta}} \tag{28}$$

$$\eta_{ij} = \frac{1}{w_i + w_{ij}} \tag{29}$$

where F_i is the neighboring list of node v_i, in the graph $G2$, while η_{ij} represents the quality of the power line (edge) e_{ij}, α and β are two parameters that control, respectively, the importance of the pheromone intensity and the quality of the power line.

5. The algorithm runs in iterations, and at each iteration an energy efficient path is selected (set S in Figure 5), and the amount of the pheromone is updated according to Equations (26) and (27).
6. The energy efficient path is the path with the minimum power transmission loss in set S (Equation (21)).

A virtual circuit, constructed using the selected energy efficient path, is allocated to transfer the power between the producer–consumer pair. The exchange information between routers during the creation of energy transmission circuits and the verification of capacity constraints before the construction of the paths prevent the congestion and overhead problems.

6. Algorithms Complexity

Algorithm complexity is one of the metrics used to measure the performance of any given algorithm. In our proposed approach, we have used ACO and PSO algorithms to obtain the best optimal solution. ACO is exploited to find the efficient paths between consumers and their producers. PSO is used to determine the best producers for a heavy load consumer. Despite the fact that the ACO algorithm presents limitations in large-scale combinatorial problems because they require huge processing time, in our case, it outperformed the greedy search algorithm used in [20] to solve the same problem. In what follows, we computed the used algorithms complexity.

We can compute the subscriber matching's complexity in two cases: heavy loaded network (ComplexHeavy) and light loaded network (ComplexNotHeavy). Since the IACO algorithm is invoked in both cases, let us compute its complexity first. Assume n is the number of ER nodes, m is the number of ants, and the maximum number of iteration is maxit. Then, the time complexity analysis of IACO algorithm is: $O(n \times (n-1) \times m \times maxit/2)$

(1) The time complexity of the light-loaded network is (see Table 7):

$$\begin{aligned} ComplexNotHeavy &= 1 + np \times (1 + comIACO + 1) + 1 \\ &= 2 + 2 \times np + np \times comIACO \\ &= 2 + 2 \times np + np \times O(n \times (n-1) \times m \times maxit/2) \\ &= O(n^2 \times m \times maxit/2) \\ &because \quad 2 + 2 \times np \quad is \quad less \quad than \quad comIACO. \end{aligned}$$

where *np* is the number of possible producers.

Table 7. Light-loaded network case.

Instruction	Complexity	Explanations
$Fitness \leftarrow 0$	O(1)	Elementary instruction
$cost_p \leftarrow calculatecost(L(i), P_c)$	O(1)	Repeated np times
$w_{c \leftrightarrow p} \leftarrow IACObasedERP(L(i), c, P_c)$	comIACO	Repeated np times
$Fitness_p(i) \leftarrow \alpha \times w_{c \leftrightarrow p} + (1-\alpha) \times Cost_p$	O(1)	Repeated np times
$Fitness = min(Fitness_p)$	O(1)	Elementary instruction

(2) The time complexity of the heavy loaded network is (the worst scenario (see Table 8)):

$$\begin{aligned} ComplexHeavy &= comp(C(c,n)) + \\ &m \times comp(EPSOA) + \\ &comp(EPSOAobjectivefunction) + 1 \\ &= O(n^{min(c,c-n)}) + m \times O(maxit \times k \times np) + O(n^2 \times m \times maxit/2) + 1 \end{aligned}$$

where:

- $comp(C(c,n)) = O(n^{min(c,c-k)})$ is the combination complexity.
- *comp(EPSOA)* is the *EPSOA* algorithm complexity. The*EPSOA* algorithm contains several elementary instructions, two nested loops and three nested loops. Then, its complexity is *O(maxit* $\times$ *k* $\times$ *np)* (see Table 9):

  $$\begin{aligned} comp(EPSOA) &= 1 + O(k \times n) + O(k) + 4 + 5 \times O(maxit) + \\ &3 \times O(k \times maxit) + 2 \times O(maxit \times k \times np) \\ &= O(maxit \times k \times np) \end{aligned}$$

  where *k* is the number of particles.
- comp(*EPSOA* objective function) is the same as the complexity of the light loaded network case, previously computed as:
  $comp(EPSOAobjectivefunction) = O(n^2 \times m \times maxit/2)$

Table 8. Heavy loaded network case.

Instruction	Complexity	Explanations
$C_n^c \leftarrow createCombination(P_c, L)$	$O(n^{min(c,c-k)})$	Combination
$Fitness_s(i) \leftarrow EPSOA(C_c^n(i), c, P_c)$	*comp(EPSOA)*	Repeated m times
$Fitness \leftarrow min(Fitness_s)$	O(1)	Elementary instruction
comp(EPSOA objective function)	$O(n^2 * m * maxit/2)$	The same as compIACO

Table 9. *EPSOA* complexity: *comp(EPSOA)*.

Instruction	Complexity	Explanations
$i \leftarrow 1$	O(1)	elementary instruction
$X(i,j) \leftarrow Rand(X(i,j)_{min}, X(i,j)_{max})$	O(k*n)	2 nested loops
while and for $f_0(i) \leftarrow OF(X(i,:), S, c)$	O(k)	Executed k times
$[f0min, index] \leftarrow min(f_0)$	O(1)	Elementary instruction
$pbest \leftarrow X$	O(1)	//
$gbest \leftarrow X(index)$	O(1)	//
$ite \leftarrow 1$	O(1)	//
Update V	*O(maxit)*	One loop while
Update X	$O(maxit * k * np)$	3 nested loops
$X(i,j) \leftarrow X(i,j) + V(i,j)$	$O(maxit * k * np)$	//
$f(i) \leftarrow OF(X(i,:), S, c)$	$O(maxit * k)$	2 nested loops
$f_0(i) \leftarrow f(i)$	$O(maxit * k)$	//
$pbest(i) \leftarrow X(i,:)$	$O(maxit * k)$	//
$[fmin, index] \leftarrow min(f_0)$	$O(maxit)$	One loop while
$gbest \leftarrow pbest(index)$	$O(maxit)$	//
$f0min \leftarrow fmin$	$O(maxit)$	//
$i \leftarrow i+1$	$O(maxit)$	//

7. Simulation and Results

In this section, various study cases, implemented in MATLAB, were conducted to validate the effectiveness of the proposed energy routing approach. Additionally, the comparison to an existing routing algorithm is carried out to evaluate the performance of the proposed approach. The ER-based EI represented in Figure 1 is treated as a simulation case where the energy system parameters are:

7.1. Basic Data

Tables 2 and 3 illustrate the parameters of power lines and ERs used in the proposed EI (Figure 1). On the other hand, Table 10 lists the energy profile of producers/consumers in the proposed network, including the cost, power and required transmission time.

Table 10. Energy profile of the system prosumers (*P*) and consumers (*C*) in different cases.

Energy Profile		*D2*	*D3*	*D4*	*D7*
C/*P*		*P*	*C*	*P*	*C*
P (Kw)		15	−9	25	−12
cost (USD/Kw.h)		0.068	-	0.043	-
Transmission Time (h:m)	Case 1	09:45–14:00	10:00–12:00	09:00–14:00	12:00–14:00
	Case 2	09:45–14:00	10:00–12:00	09:00–12:00	10:15–12:15
	Case 3	09:45–14:00	10:00–12:00	09:00–12:00	10:15–12:15

7.2. Results of the Proposed Energy Routing Approach

Applying the proposed energy routing approach, a source selection (Section 4) with a non-congestion minimum loss path (Section 5) is constructed for each consumer.

Case 1 analysis: mono-source consumer with non overlapping transmission time

In this case, according to Table 10, there are two consumers (*D7* and *D3*) with two producers (*D2* and *D4*). The transmission time of the consumers is different, which means it does not have any overlap. Thus, in this case, the pre-existing power through lines is zero and the energy transmission path taken by the first consumer will not affect the second one. Starting with consumer *D7*, using the proposed energy routing mechanism:

1. *D7* sends energy request to ER_{17}.
2. ER_{17} transfers this request to the broker.

3. The broker creates a list with the available producers that can provide 12 kw in the corresponding time (10.00–12.00) $L = \{D2, D4\}$, and sends it to ER_{17}.
4. ER_{17} starts the execution of the subscriber matching mechanism (Section 4). As we can see, *D7* is a mono-source consumer. Thus, for each producer in L (*D2* and *D4*), the ER_{17} calculates the cost and the energy-efficient path to determine the fitness value. The energy-efficient path is given by the execution of IACO-based energy routing protocol (IACO-ERP) described in Section 5. The protocol's first phase allows the ER_{17} to construct a new graph from the EI graph (Figure 2) by deleting all the lines and routers that cannot transfer 12 kw as shown in Figure 6. This step with the dynamic routing creates a non-congestion minimum loss path.
5. As described in Equation (3), in our approach, the objective was the minimization of the power loss and cost of energy. For that, the value of α used in the calculation of the fitness value was 0.5. With this value, ER_{17} selects the producer $D4$ with the fitness value for consumer $D7$.
   The same process is repeated for consumer $D3$ with ER_{10}.

The calculation results including costs, efficient paths, power losses and selected sources, transmission power and the max capacity of paths are shown in Table 11 and Figure 6. The selected producers with the efficient paths for consumer *D7* and *D3* satisfied the energy routing constraints.

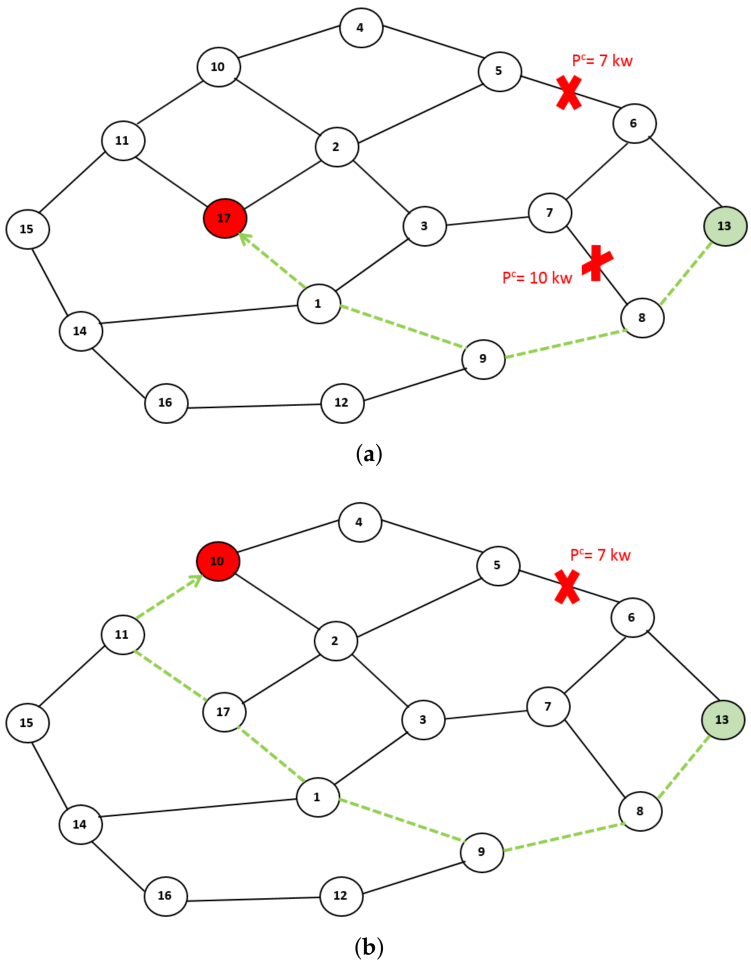

Figure 6. Optimization results of case 1 ($\alpha = 0.5$): (**a**) energy-efficient path from *D4* (ER_{13}) to *D7* (ER_{17}); (**b**) energy-efficient path from *D4* (ER_{13}) to *D3* (ER_{10}).

Table 11. The results of the energy routing approach for case 1 ($\alpha = 0.5$).

Consumer	Producer	Transaction Power (kw)	Cost (USD/kw.h)	Energy Efficient Path	Power Loss (kw)	Transmission Capacity (kw)	Fitness Value	Selected Producer
D7	*D2*	12	1.68	$9 \rightarrow 1 \rightarrow 17$	0.480621	20	1.080311	*D4*
	D4	12	1.08	$13 \rightarrow 8 \rightarrow 9 \rightarrow 1 \rightarrow 17$	0.841377	20	0.960689	
D3	*D2*	8	1.12	$9 \rightarrow 1 \rightarrow 17 \rightarrow 11 \rightarrow 10$	0.560468	20	0.840234	*D4*
	D4	8	0.72	$13 \rightarrow 8 \rightarrow 9 \rightarrow 1 \rightarrow 17 \rightarrow 11 \rightarrow 10$	0.800804	20	0.760402	

As illustrated in Figures 7 and 8, the variation of α from 0 to 1 shows that the degree of the importance of the cost and power loss progresses in the opposite direction, which affects the producer selection. There are two special cases when $\alpha = 0$ or $\alpha = 1$:

- $\alpha = 0$: The fitness value depends only on the cost of energy, in this case, the producer with the minimum fitness value is producer *D4*.
- $\alpha = 1$: The fitness value depends only on the power transmission loss of the best path, in this case, the producer with the minimum fitness value is producer *D2*.

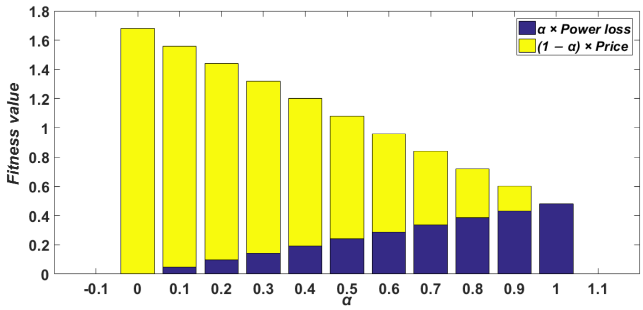

(**a**)

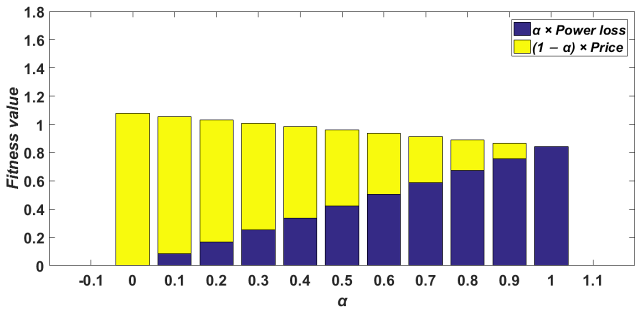

(**b**)

Figure 7. Fitness value for *D7* based on the variation of α: (**a**) for producer *D2*; (**b**) for producer *D4*.

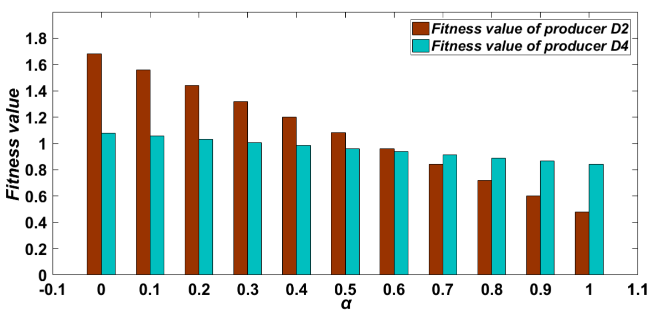

Figure 8. *D2* and *D4* Fitness values for *D7* based on α variation.

Case 2 analysis: mono-source consumer with overlapping transmission time

Consumers *D3* and *D7* have an overlapping transmission time (case 2 in Table 10). Thus, the pre-existing power over certain power lines may be different from zero. This will lead to major changes of the power loss in those lines, which directly affect the efficient path selection; therefore, affecting the fitness value responsible for the producer selection.

By comparison to case 1, as shown in Table 12 and Figure 9, the selected producer for consumer *D7* is *D4* with the same energy efficient path, power loss and fitness value since, at the beginning, the pre-existing power in this path is equal to zero. However, across the overlapping time, the energy-efficient transmission paths from *D3* to *D2* and *D4* have changed from the original paths $9 \rightarrow 1 \rightarrow 17 \rightarrow 11 \rightarrow 10$, and $13 \rightarrow 8 \rightarrow 9 \rightarrow 1 \rightarrow 17 \rightarrow 11 \rightarrow 10$, to $9 \rightarrow 1 \rightarrow 3 \rightarrow 2 \rightarrow 10$ and $13 \rightarrow 6 \rightarrow 7 \rightarrow 3 \rightarrow 2 \rightarrow 10$, respectively. Because of the change in the pre-existing power in $13 \rightarrow 8 \rightarrow 9 \rightarrow 1 \rightarrow 17$, from 0 to 12 kw, which results in increasing in the power losses of those power lines, has led to an augmentation in the power loss of the original efficient paths, which have become 5.61296×10^{-1} kw and 8.0264×10^{-1} kw, respectively, which influenced the fitness value.

The results of cases 1 and 2 demonstrated that the power loss in the power system was not only affected by the energy transmitted, but also by the pre-existing power.

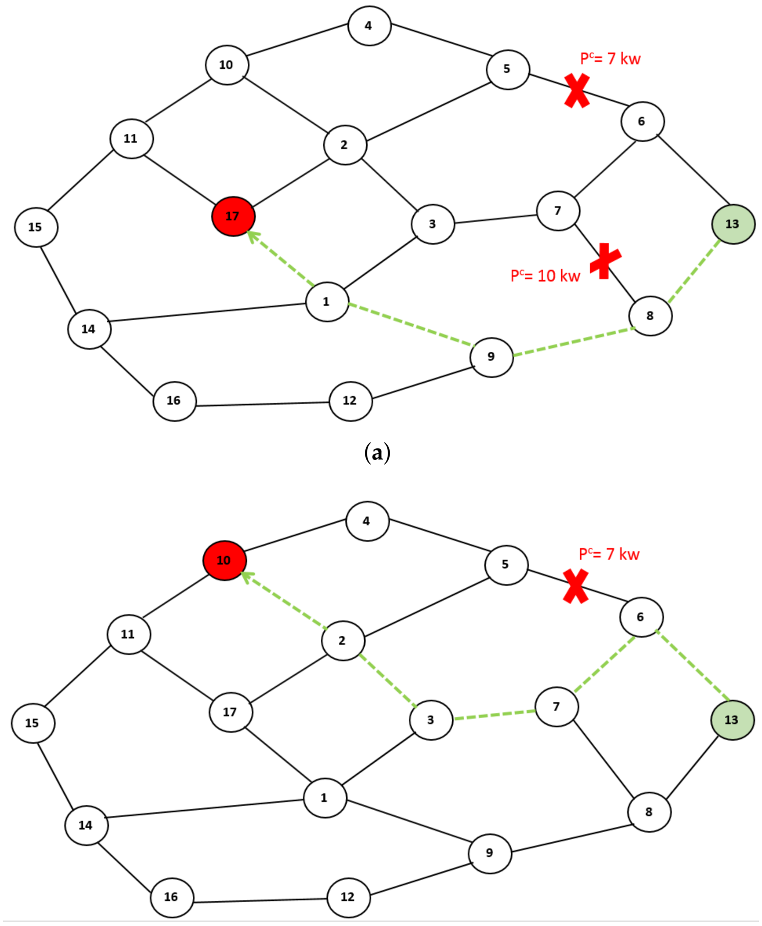

(**a**)

(**b**)

Figure 9. Optimization results of case 2 ($\alpha = 0.5$): (**a**) energy-efficient path from *D4* (ER_{13}) to *D7* (ER_{17}); (**b**) energy-efficient path from *D4* (ER_{13})to *D3* (ER_{10}).

Table 12. The results of the energy routing approach for case 2 ($\alpha = 0.5$).

Consumer	Producer	Transaction Power (kw)	Cost (USD/kw.h)	Energy Efficient Path	Power Loss (kw)	Transmission Capacity (kw)	Fitness Value	Selected Producer
D7	*D2*	12	1.68	$9 \rightarrow 1 \rightarrow 17$	0.480621	20	1.080311	*D4*
	D4	12	1.08	$13 \rightarrow 8 \rightarrow 9 \rightarrow 1 \rightarrow 17$	0.841377	20	0.960689	
D3	*D2*	8	1.12	$9 \rightarrow 1 \rightarrow 3 \rightarrow 2 \rightarrow 10$	0.561292	8	0.840646	*D4*
	D4	8	0.72	$13 \rightarrow 6 \rightarrow 7 \rightarrow 3 \rightarrow 2 \rightarrow 10$	0.800888	15	0.760444	

Case 3 analysis: congestion management

Energy transmission congestion can occur in energy systems when the transmitted power exceeds the capacity of the transmission paths, known as the overflow problem. This could have serious consequences in the energy system. As illustrated in Table 10, in this simulation case, it is assumed that there is an overlapping transmission time such as in case 2, and the capacity of power lines L_{3-7} and L_{8-13} are restricted to 12 kw and 6 kw, respectively.

As mentioned before in Section 5, the IACO-based energy routing protocol eliminates all the ERs and lines that cannot support the transmitted power from the network before finding the efficient path to avoid the overflow problem, and to ensure the selection of a non-congestion minimum loss path. Table 13 and Figure 10 summarize the results for this case. By comparison to case 2, we can state that:

- Consumers *D3* and *D7* have the same transmission power.
- For consumer *D7*, the efficient path from *D7* to *D2* is the same as in case 2. While, the path toward *D4* ($13 \rightarrow 8 \rightarrow 9 \rightarrow 1 \rightarrow 17$), cannot be used in this transaction since the transmission power (12 kw) exceeds the capacity of line L_{8-13} (6 kw). Therefore, it has been replaced by another path with higher power transmission loss, which causes an increase in the energy transmission cost.
- For consumer *D3*, as shown in Figure 10a, *D7* selected the producer *D4* with the efficient path $13 \rightarrow 6 \rightarrow 7 \rightarrow 3 \rightarrow 1 \rightarrow 17$. In this situation, the power line L_{3-7} reaches its maximum capacity, so it is not available to be shared. Therefore, ER_{10} turns from the path in case 2 ($13 \rightarrow 6 \rightarrow 7 \rightarrow 3 \rightarrow 2 \rightarrow 10$) to a new path (Table 13) with a higher loss resulting in a higher fitness value. Since consumer *D7* changed the selected path compared with case 2, this creates the opportunity to find a new path with minimal loss between *D3* and *D2* (see Table 13 and Figure 10b). As a result, *D3* turns to consumer *D2* with a minimum fitness value.

Table 13. The results of the energy routing approach for case 3 ($\alpha = 0.5$).

Consumer	Producer	Transaction Power (kw)	Cost (USD/kw.h)	Energy Efficient Path	Power Loss (kw)	Transmission Capacity (kw)	Fitness Value	Selected Producer
D7	*D2*	12	1.68	$9 \rightarrow 1 \rightarrow 17$	0.480621	15	1.080311	*D4*
	D4	12	1.08	$13 \rightarrow 6 \rightarrow 7 \rightarrow 3 \rightarrow 1 \rightarrow 17$	0.842007	12	0.961004	
D3	*D2*	8	1.12	$9 \rightarrow 1 \rightarrow 17 \rightarrow 11 \rightarrow 10$	0.560756	8	0.840378	*D2*
	D4	8	0.72	$13 \rightarrow 6 \rightarrow 7 \rightarrow 8 \rightarrow 9 \rightarrow 1 \rightarrow 17 \rightarrow 11 \rightarrow 10$	1.201820	8	0.960910	

Case 4 analysis: multi-source consumer

In order to validate the effectiveness of the proposed energy routing approach in multi-source consumer cases, we considered the electric vehicle (EV) as a heavy load with a charging request of 22 kw (according to the European EV charging standard IEC 61851 [41]). As shown in Table 14, we assume that there are three producers and none of them can provide the requested power. In this case, more than one producer should be selected to satisfy the EV demand power (*D1*). Consumer *D1* (EV) requests the required power using ER_4. In contrast to the previous cases, the broker list in this case contains all the producers that are available in the EV transmission time ($L = \{D2, D5, D6\}$). According to the power information of the producers in L, at least two sources are needed to provide the requested amount of power by the consumer. Therefore, after receiving the list ($L = \{D2, D5, D6\}$), ER_4 using Equation (6) creates a combination set as

$$C_2^{D1} = \begin{pmatrix} S_1 \\ S_2 \end{pmatrix}_{2\times1} = \begin{pmatrix} D2 & D6 \\ D5 & D6 \end{pmatrix}_{2\times2} \tag{30}$$

Table 14. Energy profile of the system producers and consumers in the case of a multi-source consumer.

Energy Profile	*D1*	*D2*	*D5*	*D6*
Consumer/Prosumer	Consumer	Producer	Prosumer	Producer
P (Kw)	−22	9	12	15
cost (USD/Kw.h)	-	0.068	0.056	0.043
Transmission Time (h:m)	11.00–12:00	10:00–12:00	09:00–14:00	12:00–14:00

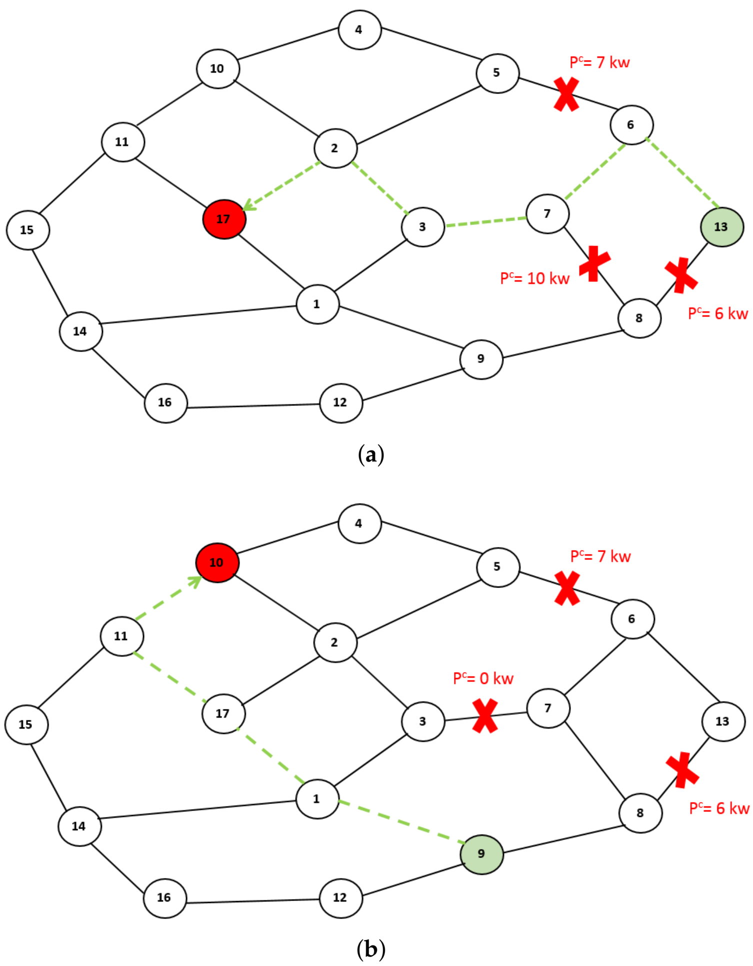

Figure 10. Optimization results of case 3 ($\alpha = 0.5$): (**a**) energy-efficient path from *D4* (ER_{13}) to *D7* (ER_{17}); (**b**) energy efficient path from *D2* (ER_9) to *D3* (ER_{10}).

There are two possible sources combination sets (S_1, S_2). According to the Equation (3), the fitness value is calculated using a function that optimizes the cost and power loss. Therefore, for each set S_i the ER_4 invokes the *EPSOA* to define the optimum amount of power that should be collected from each producer in the S_i where this amount of power optimizes the fitness value ($Fitness_{S_i}$) as well as satisfies the consumer demand.

Table 15 shows the simulation results of multi-source consumer case, however, Table 16 represents the IACO-based energy routing protocol and *EPSOA* simulation parameters.

Table 15. EPSO's results case 4 ($\alpha = 0.5$).

Set	Producer	Energy Amount (kw)	Cost (USD/kw.h)	Efficient Path	Power Loss (kw)	Transmission Capacity (kw)	Fitness Value ($Fitness_p$)	Set Fitness ($Fitness_{S_i}$)
S_1	*D2*	7	0.49	$9 \rightarrow 1 \rightarrow 3 \rightarrow 2 \rightarrow 5 \rightarrow 4$	0.420732	15	0.455366	1.39436
	D6	15	0.675	$16 \rightarrow 14 \rightarrow 15 \rightarrow 11 \rightarrow 10 \rightarrow 4$	1.202998	17	0.938991	
S_2	*D5*	11.9928	0.695582	$15 \rightarrow 11 \rightarrow 10 \rightarrow 4$	0.361114	18	0.528348	1.204567
	D6	10.0072	0.450324	$16 \rightarrow 14 \rightarrow 1 \rightarrow 3 \rightarrow 2 \rightarrow 5 \rightarrow 4$	0.902113	12.0072	0.676219	

Table 16. IACO-BERP and *EPSOA* simulation parameters.

Algorithm	Simulation Parameters			
IACO-ERP	Population size	Iteration number	α (Equation (28))	β
	10	5	1	1
EPSOA	Population size	Iteration number	*C*1	*C*2
	20	10	2	2

As shown in Table 15, the fitness value of S_1 is larger than the fitness value of S_2. Thus, ER_4 chooses the set S_2 with the power and paths allocation shown in Figure 11:

$$\begin{cases} p_{D5} &= 11.9928\,\text{kw} \quad path(D5:D1): \quad 15 \rightarrow 11 \rightarrow 10 \rightarrow \; 4 \\ p_{D6} &= 10.0072\,\text{kw} \quad path(D6:D1): \quad 16 \rightarrow 14 \rightarrow 1 \rightarrow 3 \rightarrow 2 \rightarrow 5 \rightarrow \; 4 \end{cases}$$

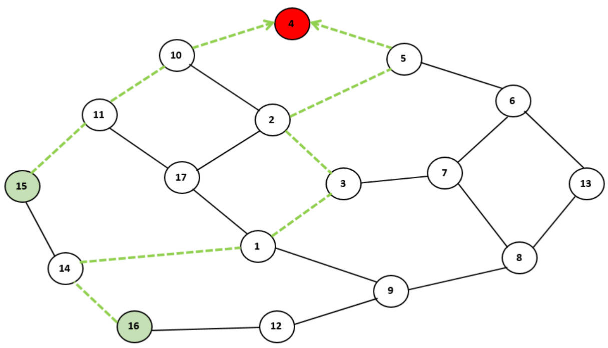

Figure 11. Optimization results of case 4 ($\alpha = 0.5$).

Tables 17–19 show the variation of α and its affect on the results of *EPSOA*. Figure 12 shows the convergence of the *EPSOA* in the two sets.

Table 17. α variation in multi-source consumer case for S_1.

	D2					D6				
α	**Energy Amount (kw)**	**Cost (USD/kw.h)**	**Efficient Path**	**Power Loss (kw)**	**Fitness Value**	**Energy Amount (kw)**	**Cost (USD/kw.h)**	**Efficient Path**	**Power Loss (kw)**	**Fitness Value**
0	7	0.49	$9 \rightarrow 1 \rightarrow 3 \rightarrow 2 \rightarrow 5 \rightarrow 4$	0.4207	0.49	15	0.675	$16 \rightarrow 14 \rightarrow 15 \rightarrow 11 \rightarrow 10 \rightarrow 4$	1.2030	0.675
0.1	7	0.49	$9 \rightarrow 1 \rightarrow 3 \rightarrow 2 \rightarrow 5 \rightarrow 4$	0.4207	0.4831	15	0.675	$16 \rightarrow 14 \rightarrow 15 \rightarrow 11 \rightarrow 10 \rightarrow 4$	1.2030	0.7278
0.2	7	0.49	$9 \rightarrow 1 \rightarrow 3 \rightarrow 2 \rightarrow 5 \rightarrow 4$	0.4207	0.4762	15	0.675	$16 \rightarrow 14 \rightarrow 15 \rightarrow 11 \rightarrow 10 \rightarrow 4$	1.2030	0.7806
0.3	7	0.49	$9 \rightarrow 1 \rightarrow 3 \rightarrow 2 \rightarrow 5 \rightarrow 4$	0.4207	0.4692	15	0.675	$16 \rightarrow 14 \rightarrow 15 \rightarrow 11 \rightarrow 10 \rightarrow 4$	1.2030	0.8334
0.4	7	0.49	$9 \rightarrow 1 \rightarrow 3 \rightarrow 2 \rightarrow 5 \rightarrow 4$	0.4207	0.4623	15	0.675	$16 \rightarrow 14 \rightarrow 15 \rightarrow 11 \rightarrow 10 \rightarrow 4$	1.2030	0.8862
0.5	7	0.49	$9 \rightarrow 1 \rightarrow 3 \rightarrow 2 \rightarrow 5 \rightarrow 4$	0.4207	0.4554	15	0.675	$16 \rightarrow 14 \rightarrow 15 \rightarrow 11 \rightarrow 10 \rightarrow 4$	1.2030	0.9390
0.6	7.9838	0.5589	$9 \rightarrow 1 \rightarrow 3 \rightarrow 2 \rightarrow 5 \rightarrow 4$	0.4800	0.5115	14.0162	0.6307	$16 \rightarrow 14 \rightarrow 15 \rightarrow 11 \rightarrow 10 \rightarrow 4$	1.1239	0.9266
0.7	7.9839	0.5589	$9 \rightarrow 1 \rightarrow 3 \rightarrow 2 \rightarrow 5 \rightarrow 4$	0.4800	0.5037	14.0162	0.6307	$16 \rightarrow 14 \rightarrow 15 \rightarrow 11 \rightarrow 10 \rightarrow 4$	1.1239	0.9760
0.8	7.9980	0.5599	$9 \rightarrow 1 \rightarrow 3 \rightarrow 2 \rightarrow 5 \rightarrow 4$	0.4808	0.4966	14.002	0.6301	$16 \rightarrow 14 \rightarrow 15 \rightarrow 11 \rightarrow 10 \rightarrow 4$	1.1228	1.0242
0.9	7.9980	0.5599	$9 \rightarrow 1 \rightarrow 3 \rightarrow 2 \rightarrow 5 \rightarrow 4$	0.4808	0.4887	14.002	0.6301	$16 \rightarrow 14 \rightarrow 15 \rightarrow 11 \rightarrow 10 \rightarrow 4$	1.1228	1.0735
1	8	0.56	$9 \rightarrow 1 \rightarrow 3 \rightarrow 2 \rightarrow 5 \rightarrow 4$	0.4810	0.4810	14	0.63	$16 \rightarrow 14 \rightarrow 15 \rightarrow 11 \rightarrow 10 \rightarrow 4$	1.1226	1.1226

Table 18. α variation in multi-source consumer case for S_2.

	D5					D6				
α	**Energy Amount (kw)**	**Cost (USD/kw.h)**	**Efficient Path**	**Power Loss (kw)**	**Fitness Value**	**Energy Amount (kw)**	**Cost (USD/kw.h)**	**Efficient Path**	**Power Loss (kw)**	**Fitness Value**
0	7	0.406	$15 \rightarrow 11 \rightarrow 10 \rightarrow 4$	0.2105	0.406	15	0.675	$16 \rightarrow 14 \rightarrow 1 \rightarrow 3 \rightarrow 2 \rightarrow 5 \rightarrow 4$	1.3533	0.675
0.1	7	0.406	$15 \rightarrow 11 \rightarrow 10 \rightarrow 4$	0.2105	0.3865	15	0.675	$16 \rightarrow 14 \rightarrow 1 \rightarrow 3 \rightarrow 2 \rightarrow 5 \rightarrow 4$	1.3533	0.7428
0.2	11.9928	0.6287	$15 \rightarrow 11 \rightarrow 10 \rightarrow 4$	0.3611	0.5284	10.0072	0.4503	$16 \rightarrow 14 \rightarrow 1 \rightarrow 3 \rightarrow 2 \rightarrow 5 \rightarrow 4$	0.9021	0.5407
0.3	11.9928	0.6287	$15 \rightarrow 11 \rightarrow 10 \rightarrow 4$	0.3611	0.5952	10.0072	0.4503	$16 \rightarrow 14 \rightarrow 1 \rightarrow 3 \rightarrow 2 \rightarrow 5 \rightarrow 4$	0.9021	0.5859
0.4	11.9928	0.6287	$15 \rightarrow 11 \rightarrow 10 \rightarrow 4$	0.3611	0.5618	10.0072	0.4503	$16 \rightarrow 14 \rightarrow 1 \rightarrow 3 \rightarrow 2 \rightarrow 5 \rightarrow 4$	0.9021	0.63104
0.5	11.9928	0.6956	$15 \rightarrow 11 \rightarrow 10 \rightarrow 4$	0.3611	0.5284	10.0072	0.4503	$16 \rightarrow 14 \rightarrow 1 \rightarrow 3 \rightarrow 2 \rightarrow 5 \rightarrow 4$	0.9021	0.6762
0.6	11.9928	0.6957	$15 \rightarrow 11 \rightarrow 10 \rightarrow 4$	0.3611	0.4949	10.0072	0.4503	$16 \rightarrow 14 \rightarrow 1 \rightarrow 3 \rightarrow 2 \rightarrow 5 \rightarrow 4$	0.9021	0.7214
0.7	11.9928	0.6956	$15 \rightarrow 11 \rightarrow 10 \rightarrow 4$	0.3611	0.4616	10.0072	0.4503	$16 \rightarrow 14 \rightarrow 1 \rightarrow 3 \rightarrow 2 \rightarrow 5 \rightarrow 4$	0.9021	0.7666
0.8	11.986	0.6952	$15 \rightarrow 11 \rightarrow 10 \rightarrow 4$	0.3609	0.4278	10.014	0.4506	$16 \rightarrow 14 \rightarrow 1 \rightarrow 3 \rightarrow 2 \rightarrow 5 \rightarrow 4$	0.9027	0.8123
0.9	11.987	0.6953	$15 \rightarrow 11 \rightarrow 10 \rightarrow 4$	0.3609	0.3944	10.013	0.4506	$16 \rightarrow 14 \rightarrow 1 \rightarrow 3 \rightarrow 2 \rightarrow 5 \rightarrow 4$	0.9026	0.8574
1	12	0.696	$15 \rightarrow 11 \rightarrow 10 \rightarrow 4$	0.3613	0.3613	10	0.45	$16 \rightarrow 14 \rightarrow 1 \rightarrow 3 \rightarrow 2 \rightarrow 5 \rightarrow 4$	0.9015	0.9015

Table 19. Set fitness.

α	$Fitness_{S_1}$	$Fitness_{S_2}$
0	1.165	1.081
0.1	1.21087	1.129274
0.2	1.25674	1.169371
0.3	1.30261	1.181103
0.4	1.34849	1.192835
0.5	1.39436	1.204567
0.6	1.43817	1.216299
0.7	1.47959	1.228031
0.8	1.52086	1.240071
0.9	1.56223	1.2518
1	1.60355	1.262795

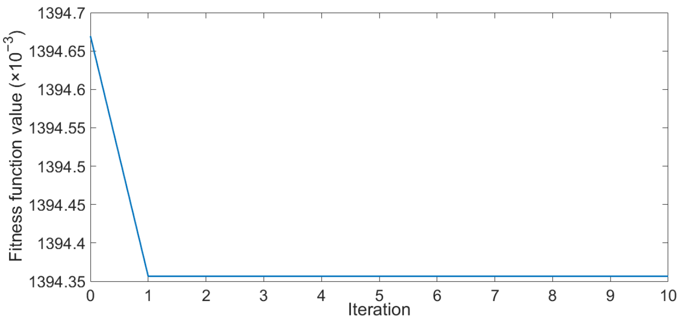

(**a**)

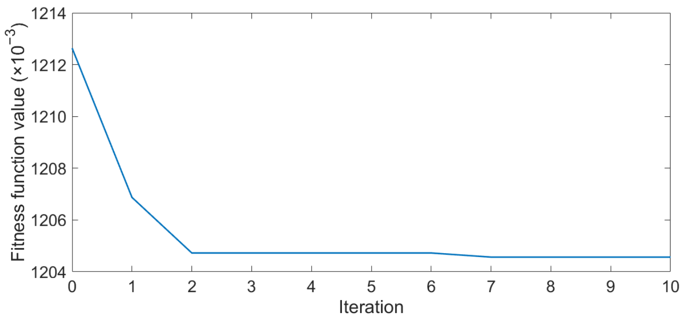

(**b**)

Figure 12. *EPSOA* convergence ($\alpha = 0.5$): (**a**) For S_1; (**b**) for S_2.

Case 5 analysis: 30 nodes system structure

The 30-node (ERs) system was used for further study to validate the efficacy of the proposed energy routing approach on a more complex system, as shown in Figure 13. Tables 20 and 21 show the power lines and ERs parameters used for system in Figure 13. In this system, there are two mono-source consumers, one multi-source consumer and four surplus-energy prosumers. Table 22 displays their energy profile including their cost, power and required transmission time.

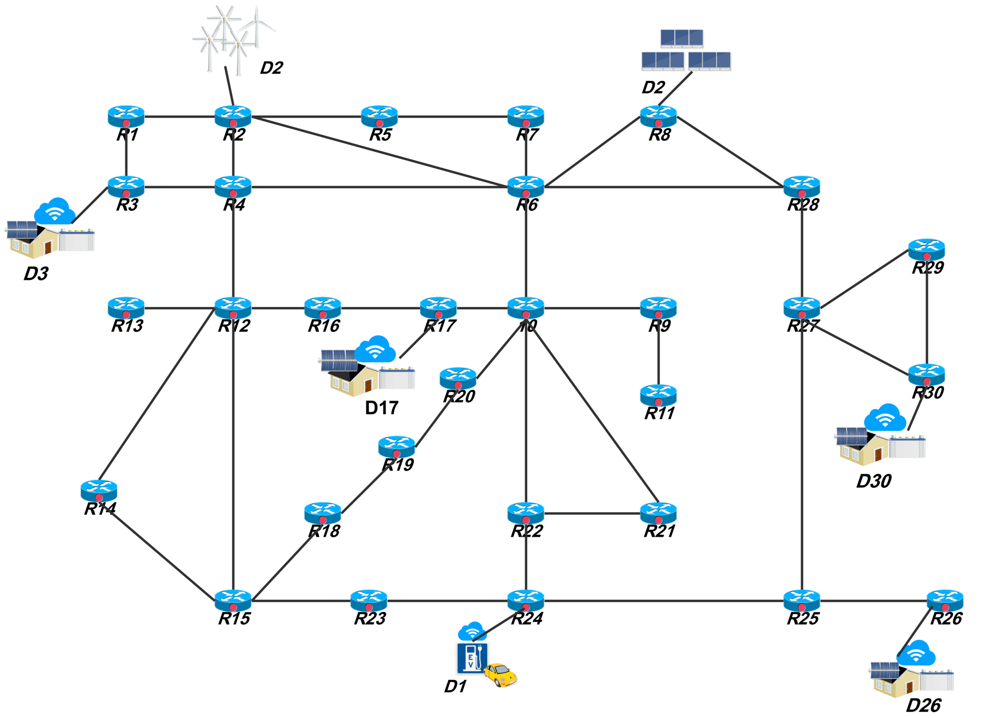

Figure 13. Thirty nodes (ER) system.

In case 1 in Table 22, the transmission time of the different consumers does not have an overlapping time. Thus, the different energy transactions will not affect each other during the selection of the minimum energy loss transmission path.

Table 23 illustrates the optimization results of the proposed approach with $\alpha = 0.5$. The constructed pairs with the transmission paths that all energy routing constraints such as the power loss and capacity constraints.

Table 20. Energy information of ERs for Figure 13.

ER	Interface Capacity (kw)	Conversion Efficiency (*eff*)	ER	Interface Capacity (kw)	Conversion Efficiency (*eff*)
R_1	30	1	R_{16}	19	0.97
R_2	35	0.98	R_{17}	15	0.98
R_3	25	1	R_{18}	30	1
R_4	45	1	R_{19}	22	1
R_5	25	0.98	R_{20}	18	0.97
R_6	40	0.97	R_{21}	15	0.98
R_7	25	0.98	R_{22}	40	0.97
R_8	20	0.97	R_{23}	25	0.97
R_9	25	0.98	R_{24}	40	0.98
R_{10}	30	0.97	R_{25}	30	1
R_{11}	22	1	R_{26}	25	1
R_{12}	22	0.98	R_{27}	40	0.97
R_{13}	25	1	R_{28}	45	0.98
R_{14}	18	0.98	R_{29}	30	0.98
R_{15}	15	1	R_{30}	30	0.98

Table 21. Energy information of power lines connecting ERs for Figure 13.

Power Line	Capacity P_{line}^{C} (kw)	Resistance (Ω)	Voltage (V)	Power Line	Capacity P_{line}^{C} (kw)	Resistance (Ω)	Voltage (V)
L_{1-2}	30	0.6	400	L_{10-22}	35	0.19	400
L_{1-3}	18	0.45	400	L_{12-13}	30	0.6	400
L_{2-4}	45	0.64	400	L_{12-14}	20	0.24	400
L_{2-5}	20	0.51	400	L_{12-15}	22	0.21	400
L_{2-6}	15	0.19	400	L_{12-16}	10	0.54	400
L_{3-4}	25	0.94	400	L_{14-15}	15	0.19	400
L_{4-6}	15	0.21	400	L_{15-18}	32	0.51	400
L_{4-12}	19	0.45	400	L_{15-23}	18	0.6	400
L_{5-7}	18	2.24	400	L_{16-17}	30	0.64	400
L_{6-7}	24	0.51	400	L_{18-19}	40	0.24	400
L_{6-8}	17	0.24	400	L_{19-20}	20	0.51	400
L_{6-9}	35	0.6	400	L_{21-22}	30	0.6	400
L_{6-10}	40	0.64	400	L_{22-24}	45	0.24	400
L_{6-28}	17	0.45	400	L_{23-24}	22	0.45	400
L_{8-28}	40	0.64	400	L_{24-25}	12	0.6	400
L_{9-10}	30	0.51	400	L_{25-26}	20	0.51	400
L_{9-11}	25	0.24	400	L_{25-27}	15	0.19	400
L_{10-17}	25	0.21	400	L_{27-28}	25	0.45	400
L_{10-20}	15	0.94	400	L_{27-29}	8	0.6	400
L_{10-21}	18	0.45	400	L_{27-30}	20	0.24	400
L_{29-30}	30	0.51	400				

Table 22. Energy profile of system prosumers (P) and consumers (C) for Figure 13.

Energy Profile		*D2*	*D3*	*D8*	*D17*	*D24*	*D26*	*D30*
C/P		*P*	*P*	*P*	*C*	*C*	*C*	*P*
P (Kw)		12	7	17	−5	−22	−6	7
cost (USD/Kw.h)		0.056	0.068	0.041	-	-	-	0.043
Transmission Time (h:m)	case 1	11:00 15:30	08:00 15:00	09:45 15:00	12:45 14:45	11:30 12:30	08:00 10:00	8:00 11:00
	case 2	8:15 12:30	08:00 15:00	08:00 14:00	09:00 11:00	08:30 09:30	08:00 10:00	8:00 11:00

However, in case 2 in Table 22, there is an overlapping time between the transmission time of consumers. Consumer $D26$ was supplied by producer $D30$ through the same energy-efficient path as in case 1 ($30 \rightarrow 27 \rightarrow 25 \rightarrow 26$). In this case, the left capacity in the power line was $L_{27-25} = 9$ kw and it cannot be used to transfer the required energy (see case 1 in Table 23) from prosumer $D8$ to consumer $D24$. Thus, another non-congestion energy-efficient path with a different energy amount was constructed using *EPSOA* and the IACO in set S_1 for consumer $D24$. Since the new solution for set S_1 has higher fitness function, the selected set for consumer $D24$ is set $S2$. For consumer $D7$, the only prosumer that can provide the demand in the corresponding time is $D2$.

Table 23. The results of the energy routing approach for case 5 ($\alpha = 0.5$).

	Consumer	Prosumer P	Transaction Power (kw)	Cost (USD/kw.h)	Energy Efficient Path	Power Loss (kw)	Transmission Capacity (kw)	Fitness Value	Selected Producer
Case 1: non-overlapping time	*D26*	*D30*	6	0.54	30 → 27 → 25 → 26	0.300212	15	0.420106	*D30*
		D3	6	0.84	3 → 4 → 12 → 15 → 23 → 24 → 25 → 26	0.420846	12	0.630423	
	D24	*D8*	11.95	0.513852	8 → 28 → 27 → 25 → 24	1.19668	12	0.855267	S_1
		D2	10.05	0.582897	2 → 4 → 12 → 15 → 23 → 24	0.905979	15	0.744438	
		D8	15.0584	0.647512	8 → 6 → 10 → 22 → 24	2.11003	17	1.37877	
		D3	6.94159	0.485911	3 → 4 → 12 → 15 → 23 → 24	0.486709	15	0.48631	
	D17	*D8*	5	0.43	8 → 6 → 10 → 17	0.550170	15	0.490085	*D8*
		D3	5	0.70	3 → 4 → 12 → 16 → 17	0.350402	10	0.525201	
Case 2: overlapping time	*D26*	*D30*	6	0.54	30 → 27 → 25 → 26	0.300212	15	0.420106	*D30*
		D3	6	0.84	3 → 4 → 12 → 15 → 23 → 24 → 25 → 26	0.420846	12	0.630423	
	D24	*D8*	13.9726	0.600822	8 → 6 → 10 → 22 → 24	1.95776	17	1.27929	S_2
		D2	8.0274	0.465589	2 → 4 → 12 → 15 → 23 → 24	0.723412	15	0.5945	
		D8	15.0199	0.645855	8 → 6 → 10 → 22 → 24	2.10463	17	1.37524	
		D3	6.98012	0.488608	3 → 4 → 12 → 15 → 23 → 24	0.489415	15	0.489012	
	D17	*D2*	5	0.58	2 → 4 → 12 → 16 → 17	0.450551	10	0.515276	*D2*

7.3. Results Discussion

In order to validate the performance of our proposed scheme, as well as to show its efficiency in solving problems related to energy routing, namely subscriber matching, efficient routing path and transmission scheduling, we compared the obtained results of different experiments to previous works in the literature.

As illustrated in Table 24, starting with the mono-source consumer case, works in [20,21] have proposed an energy routing protocols based on graph traversal and Dijkstra algorithms, respectively, to determine a non congestion minimum loss path between producer–consumer pairs. First, the two proposed protocols did not examine how pairs were formed. The graph traversal method in [20] finds that all possible paths between the producer and consumer pairs then determines the path with the minimum power loss. This method generates an optimal solution but with a height execution time especially in the case of large-scale networks. IACO-ERP offers the best solution compared to [20] with the same execution time for small-scale networks and a better execution time for large-scale networks as shown in Table 25. In addition, we proposed a subscriber matching mechanism that decides which producer should be chosen for the consumer while reducing the costs and losses of energy.

Table 24. Proposed approach vs. previous works.

Criteria	**Reproduced from [20], 2017**	**Reproduced from [21], 2018**	**Our Proposed Approach**
Subscriber matching			✓
Energy efficient path	✓	✓	✓
Transmission scheduling	✓	✓	✓
Mono-source consumer	✓	✓	✓
Multi-source consumer	✓		✓
Power loss	✓	✓	✓
Cost			✓

Table 25. Execution time for IACO-ERP vs Reproduced from [20], IEEE: 2017.

	Case 1		**Mono-Consumer**	**Mono-Consumer**
	D4 $\rightarrow$ ***D7***	***D2*** $\rightarrow$ ***D7***	**(30 Nodes)**	**(50 Nodes)**
[20]	0.48 s	0.50 s	36.38 s	52 s
IACO-ERP	0.67 s	0.84 s	3.51 s	6 s

For the multi-source consumer, the work in [20] proposed a source selection algorithm that determines the amount of power to obtain from each producer to satisfy the heavy load demand. The proposed algorithm used the greedy search topology where it tests all possible (interval values) cases to define the appropriate amount of power that needs to be received from each producer in the aim of minimizing the power loss. This method provides a solution with a high execution time which speedily augments with the growing of the system. The execution time of cases 4 and 5 is 217 s and 513 s, respectively, whereas using the *EPSOA* algorithm helped in achieving the best solution in a significantly reduced time while minimizing the cost and power loss at the same time. Our proposed scheme produced the same result for cases 4 and 5 in 51 s and 109 s seconds of execution time, respectively. In comparison with fully distributed peer–peer energy trading, the use of the broker minimized the number of exchange messages in the system.

8. Conclusions and Future Work

With the expanded use of renewable energy sources in EI, the centralized energy supply mode has shifted to a multi-source and multi path mode leading to the peer-to-peer energy trading market. The energy routing process is one of the major problems faced in EI. To solve this problem, we proposed a solution to the three issues: subscriber matching, energy-efficient path and transmission scheduling. For this purpose, we developed a centralized peer-to-peer energy trading scheme that uses a central broker and novel energy routing approach. The energy routing approach is based on meta-heuristic method to achieve a P2P energy trading with an efficient routing in the EI with respect to the energy routing constraints and congestion. The main objective of the proposed approach is to reduce the energy cost and losses while satisfying the consumers request. The use of a meta-heuristic method reduces the execution time. In fact, the energy routing approach is composed of three algorithms, the first one is the subscriber matching mechanism that determines the producer–consumer pairs with the minimization of the cost and losses of energy for both mono and multi-source consumers. The non-congestion energy minimum loss path between producer–consumer pairs is generated by the IACO-ERP. In the case of multi-source consumers such as EVs where none of the existing producers can provide the required energy, two or more producers should be selected to supply the requested amount of power. For that, the *EPSOA* determines the appropriate producers to achieve the lowest energy cost and losses. The effectiveness of the proposed approach, in terms of cost, power losses and congestion management, is verified by different cases analysis. The overlapping time provides a better utilization of network power lines with more power losses compared to the non-overlapping time. In addition, the use of the broker decreases the number of messages exchanged in the network. By comparison to the work in [20], our proposed approach has improved the execution time for both mono- and multi-sources cases in small and large systems by 7 min. The proposed approach can be used to match prosumers in the local energy market, provide alternative transmission paths when the efficient path is disrupted, and manage congestion on distribution links.

In the future, we plan to explore the possibility of applying additional bio-inspired methods, and we aim to explore to apply our solution to real life applications.

Author Contributions: The specific contributions made by each author are shown as follows: conceptualization, D.M.; formal analysis, S.H. (Sara Hebal); methodology, S.H. (Sara Hebal); software, S.H. (Sara Hebal); supervision, S.H. (Saad Harous); visualization, M.D.; writing—original draft, S.H. (Sara Hebal); writing—review and editing, D.M. All authors have read and agreed to the published version of the manuscript.

Funding: This research received no external funding.

Institutional Review Board Statement: Not applicable.

Informed Consent Statement: Not applicable.

Data Availability Statement: No new data were created or analyzed in this study. Data sharing is not applicable to this article.

Conflicts of Interest: The authors declare no conflict of interest.

Abbreviations

The following abbreviations were used in this manuscript:

ACO	Ant Colony Optimization
DREs	Distributed Renewable Energy sources
EI	Energy Internet
EPSOA	Energy Particle Swarm Optimization Algorithm.
ER	Energy Router
HVAC	High Voltage Alternating Current
IACO-ERP	Improved Ant Colony Optimization Energy Routing Protocol.
LVDC	Low Voltage Direct Current
MVDC	Medium Voltage Direct Current
PSO	Particle Swarm Optimization
SG	Smart Grid
SST	Solid State Transformer

References

1. Tushar, W.; Chai, B.; Yuen, C.; Smith, D.B.; Wood, K.L.; Yang, Z.; Poor, H.V. Three-party energy management with distributed energy resources in smart grid. *IEEE Trans. Ind. Electron.* **2014**, *62*, 2487–2498. [CrossRef]
2. Wang, K.; Yu, J.; Yu, Y.; Qian, Y.; Zeng, D.; Guo, S.; Xiang, Y.; Wu, J. A survey on energy internet: Architecture, approach, and emerging technologies. *IEEE Syst. J.* **2017**, *12*, 2403–2416. [CrossRef]
3. Surani, R.R. From Smart Grids to an Energy Internet: A Review Paper on Key Features of an Energy Internet. *Int. J. Eng. Res. Technol.* **2019**, *8*, 228–231.
4. Rifkin, J. *The Third Industrial Revolution: How Lateral Power Is Transforming Energy, the Economy, and the World*; Macmillan: Stuttgart, Germany, 2011.
5. Chen, Z.; Liu, Q.; Li, Y.; Liu, S. Discussion on energy internet and its key technology. *J. Power Energy Eng.* **2017**, *5*, 1–9. [CrossRef]
6. Tsoukalas, L.; Gao, R. From smart grids to an energy internet: Assumptions, architectures and requirements. In Proceedings of the 2008 Third International Conference on Electric Utility Deregulation and Restructuring and Power Technologies, Nanjing, China, 6–9 April 2008; pp. 94–98.
7. Zhou, Y.; Wu, J.; Long, C.; Ming, W. State-of-the-art analysis and perspectives for peer-to-peer energy trading. *Engineering* **2020**, *6*, 739–753. [CrossRef]
8. Cui, C.X. *The UK Electricity Markets: Its Evolution, Wholesale Prices and Challenge of Wind Energy*; University of Stirling: Stirling, UK, 2010.

9. Ye, L.C.; Rodrigues, J.F.; Lin, H.X. Analysis of feed-in tariff policies for solar photovoltaic in China 2011–2016. *Appl. Energy* **2017**, *203*, 496–505. [CrossRef]
10. Wu, J.; Zhou, W.; Zhong, W.; Liu, J. Multi-energy demand response management in energy Internet: A stackelberg game approach. *Chin. J. Electron.* **2019**, *28*, 640–644. [CrossRef]
11. Irtija, N.; Sangoleye, F.; Tsiropoulou, E.E. Contract-Theoretic Demand Response Management in Smart Grid Systems. *IEEE Access* **2020**, *8*, 184976–184987. [CrossRef]
12. Tushar, W.; Saha, T.K.; Yuen, C.; Smith, D.; Poor, H.V. Peer-to-peer trading in electricity networks: An overview. *IEEE Trans. Smart Grid* **2020**, *11*, 3185–3200. [CrossRef]
13. Abdella, J.; Shuaib, K. Peer to peer distributed energy trading in smart grids: A survey. *Energies* **2018**, *11*, 1560. [CrossRef]
14. Zhang, C.; Wu, J.; Zhou, Y.; Cheng, M.; Long, C. Peer-to-Peer energy trading in a Microgrid. *Appl. Energy* **2018**, *220*, 1–12. [CrossRef]
15. Wang, N.; Xu, W.; Xu, Z.; Shao, W. Peer-to-peer energy trading among microgrids with multidimensional willingness. *Energies* **2018**, *11*, 3312. [CrossRef]
16. Shrestha, A.; Bishwokarma, R.; Chapagain, A.; Banjara, S.; Aryal, S.; Mali, B.; Thapa, R.; Bista, D.; Hayes, B.P.; Papadakis, A.; et al. Peer-to-peer energy trading in micro/mini-grids for local energy communities: A review and case study of Nepal. *IEEE Access* **2019**, *7*, 131911–131928. [CrossRef]
17. Tushar, W.; Yuen, C.; Saha, T.K.; Morstyn, T.; Chapman, A.C.; Alam, M.J.E.; Hanif, S.; Poor, H.V. Peer-to-peer energy systems for connected communities: A review of recent advances and emerging challenges. *Appl. Energy* **2021**, *282*, 116131. [CrossRef]
18. Huang, A.Q. Solid state transformers, the Energy Router and the Energy Internet. In *The Energy Internet*; Elsevier: Amsterdam, The Netherlands, 2019; pp. 21–44.
19. Guo, H.; Wang, F.; Zhang, L.; Luo, J. A hierarchical optimization strategy of the energy router-based energy Internet. *IEEE Trans. Power Syst.* **2019**, *34*, 4177–4185. [CrossRef]
20. Wang, R.; Wu, J.; Qian, Z.; Lin, Z.; He, X. A graph theory based energy routing algorithm in energy local area network. *IEEE Trans. Ind. Inform.* **2017**, *13*, 3275–3285. [CrossRef]
21. Guo, H.; Wang, F.; James, G.; Zhang, L.; Luo, J. Graph theory based topology design and energy routing control of the energy internet. *IET Gener. Transm. Distrib.* **2018**, *12*, 4507–4514. [CrossRef]
22. Lin, J.; Yu, W.; Griffith, D.; Yang, X.; Xu, G.; Lu, C. On distributed energy routing protocols in the smart grid. In *Software Engineering, Artificial Intelligence, Networking and Parallel/Distributed Computing*; Springer: Berlin/Heidelberg, Germany, 2013; pp. 143–159.
23. Sivanantham, G.; Gopalakrishnan, S. A Stackelberg game theoretical approach for demand response in smart grid. *Pers. Ubiquitous Comput.* **2019**, *24*, 511–518. [CrossRef]
24. Apostolopoulos, P.A.; Tsiropoulou, E.E.; Papavassiliou, S. Demand response management in smart grid networks: A two-stage game-theoretic learning-based approach. *Mob. Netw. Appl.* **2018**, 1–14. [CrossRef]
25. Hong, J.S.; Kim, M. Game-theory-based approach for energy routing in a smart grid network. *J. Comput. Netw. Commun.* **2016**, *2016*, 4761720. [CrossRef]
26. Ma, J.; Song, L.; Li, Y. Optimal power dispatching for local area packetized power network. *IEEE Trans. Smart Grid* **2017**, *9*, 4765–4776. [CrossRef]
27. Tushar, W.; Saha, T.K.; Yuen, C.; Morstyn, T.; Poor, H.V.; Bean, R. Grid influenced peer-to-peer energy trading. *IEEE Trans. Smart Grid* **2019**, *11*, 1407–1418. [CrossRef]
28. Tushar, W.; Saha, T.K.; Yuen, C.; Azim, M.I.; Morstyn, T.; Poor, H.V.; Niyato, D.; Bean, R. A coalition formation game framework for peer-to-peer energy trading. *Appl. Energy* **2020**, *261*, 114436. [CrossRef]
29. Brocco, A. Fully distributed power routing for an ad hoc nanogrid. In Proceedings of the 2013 IEEE International Workshop on Inteligent Energy Systems (IWIES), Vienna, Austria, 14 November 2013; pp. 113–118.
30. Lin, C.C.; Wu, Y.F.; Liu, W.Y. Optimal sharing energy of a complex of houses through energy trading in the Internet of energy. *Energy* **2021**, *220*, 119613. [CrossRef]
31. Hebal, S.; Mechta, D.; Harous, S. ACO-based Distributed Energy Routing Protocol In Smart Grid. In Proceedings of the 2019 IEEE 10th Annual Ubiquitous Computing, Electronics & Mobile Communication Conference (UEMCON), New York, NY, USA, 10–12 October 2019; pp. 0568–0571.
32. Hebal, S.; Harous, S.; Mechta, D. Latency and Energy Transmission Cost Optimization using BCO-aware Energy Routing for Smart Grid. In Proceedings of the 2020 International Wireless Communications and Mobile Computing (IWCMC), Limassol, Cyprus, 15–19 June 2020; pp. 1170–1175. [CrossRef]
33. Mechta, D.; Harous, S.; Hebal, S. Energy-efficient path-aware routing Protocol based on PSO for Smart Grids. In Proceedings of the 2020 IEEE International Conference on Electro Information Technology (EIT), Chicago, IL, USA, 31 July–1 August 2020; pp. 093–097. [CrossRef]
34. Dhriyyef, M.; El Mehdi, A.; Elhitmy, M.; Elhafyani, M. Management strategy of power exchange in a building between grid, photovoltaic and batteries. In *International Conference on Electronic Engineering and Renewable Energy*; Springer: Singapore, 2020; pp. 831–841.
35. Liu, Y.; Li, Y.; Liang, H.; He, J.; Cui, H. Energy routing control strategy for integrated microgrids including photovoltaic, battery-energy storage and electric vehicles. *Energies* **2019**, *12*, 302. [CrossRef]

36. Liu, Y.; Wu, Y.; Yang, K.; Bi, C.; Chen, X.; Zhao, Y. Novel Energy Router with Multiple Operation Modes. *Energy Procedia* **2019**, *158*, 2586–2591. [CrossRef]
37. Guo, H.; Wang, F.; Luo, J.; Zhang, L. Review of energy routers applied for the energy internet integrating renewable energy. In Proceedings of the 2016 IEEE 8th International Power Electronics and Motion Control Conference (IPEMC-ECCE Asia), Hefei, China, 22–26 May 2016; pp. 1997–2003.
38. Huang, A.Q.; Crow, M.L.; Heydt, G.T.; Zheng, J.P.; Dale, S.J. The future renewable electric energy delivery and management (FREEDM) system: The energy internet. *Proc. IEEE* **2010**, *99*, 133–148. [CrossRef]
39. Razi, R.; Pham, C.; Hably, A.; Bacha, S.; Tran, Q.T.; Iman-Eini, H. A Novel Graph-based Routing Algorithm in Residential Multi-Microgrid Systems. *IEEE Trans. Ind. Inform.* **2020**, *17*, 1774–1784. [CrossRef]
40. Dorigo, M.; Birattari, M. *Ant Colony Optimization. Encyclopedia of Machine Learning*; Springer: New York, NY, USA, 2010.
41. Falvo, M.C.; Sbordone, D.; Bayram, I.S.; Devetsikiotis, M. EV charging stations and modes: International standards. In Proceedings of the 2014 International Symposium on Power Electronics, Electrical Drives, Automation and Motion, Ischia, Italy, 18–20 June 2014; pp. 1134–1139.